# Geomorphological Behaviour of Fetch-Limited Barrier Islands in the Laguna Madre de Tamaulipas, Mexico

## Contents

## Abstract

Fetch-Limited Barrier Islands are little studied coastal landforms. They appear in sheltered, low-energy environments worldwide, often anchored by mangroves or salt marshes, or behind their larger oceanic cousins, open-ocean barriers. This study aims to identify the processes involved in the evolution of FLBIs in the Laguna Madre de Tamaulipas, Mexico, and to critically assess their long-term stability and resilience to climate change and anthropic pressures. Satellite images from Google earth engine were processed by the software CoastSat and input into GIS software to identify yearly shoreline positions. Ten islands were measured from their earliest date to provide a series of shoreline positions. Shorelines were examined for migration, change in profile, and their overall trends in order to provide measures of variability. Islands of the same type displayed similar trends, even when differing in their levels of advance/retreat. FLBIs are shown to be highly dependent on the sediment supply available to them, being worked and reworked by seasonal storms and by locally generated wind waves. They often breach and become inundated, making the vast majority of them unsuitable for human development. Sea level rise is not found to be a factor in these islands' previous evolution and geomorphological development; however, it is understood that it remains a potential issue in regards to their future resilience. As this study was limited to satellite imagery, further in-depth field studies could provide a more detailed evaluation of these islands' behaviour and their role in the area as a whole, the habitats it contains, and the impact of human exploitation.

## 1. Introduction

Barrier Islands are coastal landforms providing protection and shelter for the mainland from wave and tidal processes. There are 2,200 ocean-facing barrier islands throughout the world, covering a total of 20,000 km (Cooper, 2012). These islands are well documented and studied as significant landforms (Stutz and Pilkey, 2011). On the contrary, fetch-limited barrier islands (FLBI) have been rarely studied and until recently, were not even recognized as a significant landform, though they cover more total surface area than ocean-facing barrier islands (Cooper et al., 2007). Around 15,000 FLBIs have been identified globally (Cooper et al 2007; Pilkey et al., 2009).

FLBIs differ from their oceanic counterparts in two major ways (Pilkey, et al., 2009):

1. The FLBI's shape and location are often controlled by the presence of salt marshes or mangroves.
2. FLBI evolution is storm driven as opposed to tidal or aeolian processes.

There are several other differences to note. The average FLBI is around 1 km in length and 10 - 100 m wide, far smaller than its oceanic counterpart. Oceanic barrier islands usually display a well-defined shoreface, with significant dune structure whereas FLBIs have a varied shoreface, or sometimes none. Dunes are often underdeveloped or absent. FLBIs average 1 to 3 m in height, much lower than ocean-facing barrier islands. FLBIs form much the same way as oceanic barrier islands, but with overwash being the most significant island building process in the FLBI (Pilkey, et al., 2009).

Around 70% of FLBIs form on trailing edge coasts due to the potential formation of sheltered waters (Pilkey, et al., 2009). For a FLBI to form there must be a low energy setting, making these sheltered waters ideal. The fetch distance for wind generated waves is generally <25km (Cooper et al., 2007). 50% of FLBIs have been identified around the coastal zones of Australia, Mexico and Russia (Cooper et al., 2007).

FLBIs can be divided into 3 broad classes regarding their evolution: active; inactive; and anthropic (Pilkey et al., 2009). Active islands continue to evolve, due to the most dominant factors being marine processes and storm events. Inactive islands are not currently being modified by these processes, and have usually been surrounded by salt marsh. Change is usually dictated by sub-aerial processes. Anthropic islands have been formed entirely by humans, usually as dredge spoil islands, ballast piles, causeways, foul piles, and artificial reefs. These islands can be difficult to separate from those which occur naturally. However, the beginnings of such islands can be affected by natural processes and eventually transform them into natural FLBIs, just as naturally occurring FLBIs can be influenced by human actions (Pilkey et al., 2009).

Further to this classification, Pilkey et al (2009) identify 8 sub-classes based upon the geomorphic setting and general morphology. These are: Classic; Two-sided; Backbarrier-parallel (BBP); Inlet; Marsh fringe; Deltaic; Fjord-head; and Thermokarst. Classic are the most abundant, representing around half of all FLBIs with an “open water” and “quiet water” side. They share similarities with open-ocean coastal plain barrier islands; however, their evolution is often greatly influenced by vegetation. Some islands can be intermittent; they are only surrounded by water during storm surges, spring tides or high tides. Two-sided are similar to Classic, differing in that they have a similar fetch in two directions. This gives a symmetrical look to both sides. They are also one of the least common, representing under 2% of the world’s total. Backbarrier-parallel make up around 8%. These islands always occur in tideless or microtidal lagoons and are formed from overwash from the oceanic barrier when it is reworked by lagoonal waves. They form long, parallel chains to the landward side of open-ocean barriers. Deltaic barrier islands form along the edge of river deltas that empty into fetch-

limited areas, developing into short chains. The fluvial sediments are manipulated by storm-generated wave setup and alongshore transport, forming islands. Fjord-head barrier islands usually form in chains of 2-4 islands, at the margin of a sandur plain, seaward of an active glacier. They are similar to deltaic and are the least common, representing 1.3%. Inlet barrier islands develop immediately behind the inlets of open-ocean barriers, on flood tidal deltas within lagoons (Pilkey et al., 2009). They almost always occur individually, but through inlet migration new islands can form, creating chains. The dunes on these islands are typically more developed than most FLBIs. A study conducted by Seymour et al (2019) suggests however, that Inlet Barrier Islands do not adhere to the FLBI archetype completely in that they can be affected by predominant conditions. Marsh fringe islands develop under the lowest energy conditions and account for 8.3% of worldwide FLBIs. They are among the smallest and show multiple planforms. Thermokarst form as permafrost tundra erodes and deposits in a fetch-limited area. They occur exclusively in Russia and North America along their Arctic coasts. They lack height (measuring only 1-2 m) and dunes, and have poorly sorted beachfaces. They are longest on average at 1.5 km and account for 16% of global distribution of FLBIs, making them the second most abundant.

Otvos (2010) argues that Pilkey et al's (2009) definition of FLBIs is flawed in that the islands do not perform the function of "barriers" and that the term "fetch-limited" would only apply to the "classic" island. Cooper et al (2011) counterargue that the islands perform a barrier function, simply on a smaller scale and that Otvos (2010) cannot accept only "classic" types and dismiss the others without suggesting an alternative classification.

Open-ocean barrier islands such as the Miami Beach barrier island complex (Zhang and Leatherman, 2011) are populated and significant development has taken place (Ehlen et al., 2005). Currently, FLBIs rarely contain human structures save for perhaps fishing huts. This is largely due to their restricted size and lower elevation when compared to their oceanic cousins. As development continues and space decreases however, attention will undoubtedly turn towards development of FLBIs (Pilkey et al., 2009). Attempts to engineer these islands for human development could have catastrophic effects (Zhang and Leatherman, 2011). Coupled with a rise in sea level, FLBIs could face a significant risk of complete disintegration (Cooper, 2013) and as such, further research into their geomorphological behaviour is vital, as rates and patterns of geomorphic change on FLBIs have been little studied.

## 2. Methodology

The aim of this research is to identify temporal geomorphological patterns and behaviours of FLBIs along the Laguna Madre de Tamaulipas. It is a hypersaline coastal lagoon and the only one on the continent of North America, and one of only five worldwide (Judd and Tunnell,

2002), and contains the highest number and density of FLBIs of any water body worldwide (Pilkey et al., 2009).

The objectives of this study are to:

1. Identify FLBIs and their sub-types within the study area.
2. Identify temporal change in FLBIs and quantify it where possible.
3. Identify possible the processes involved in geomorphological change.
4. Critically assess the resilience of FLBIs regarding climatic conditions and possible anthropic pressures.

A range of sites in the low-energy, bar-built coastal lagoon Laguna Madre de Tamaulipas (Judd and Tunnell, 2002) were examined and investigated for temporal geomorphological changes in FLBIs. The target area began in the Northern section, at the Rio Grande river delta and ended at the Soto La Marina River mouth (Figure 1).

This was achieved using secondary satellite data from Google Earth Pro and Google Earth Engine. FLBIs were identified based on previous studies such as Pilkey et al (2009) and Cooper, Lewis and Pilkey (2007). Google Earth Pro was employed to identify islands and their geographic coordinates for input into a software package. The overall study area was divided into three sectors (figure 2), measuring around 85km each from north to south. A single island of each type was identified and chosen from each area. This was done to ensure that the islands chosen were not clustered around the same area, giving a better dispersion of samples.

An island was chosen when it:

1. Was considered currently active (i.e. currently changing size and shape over time).
2. Had an image clear enough, separated from its surroundings, meaning it could be identified by a software package.
3. Provided a temporal resolution of at least 15 years prior to 2019.
4. Occurred naturally (i.e. not formed from anthropic sources such as dredge spoil and artificial reefs).

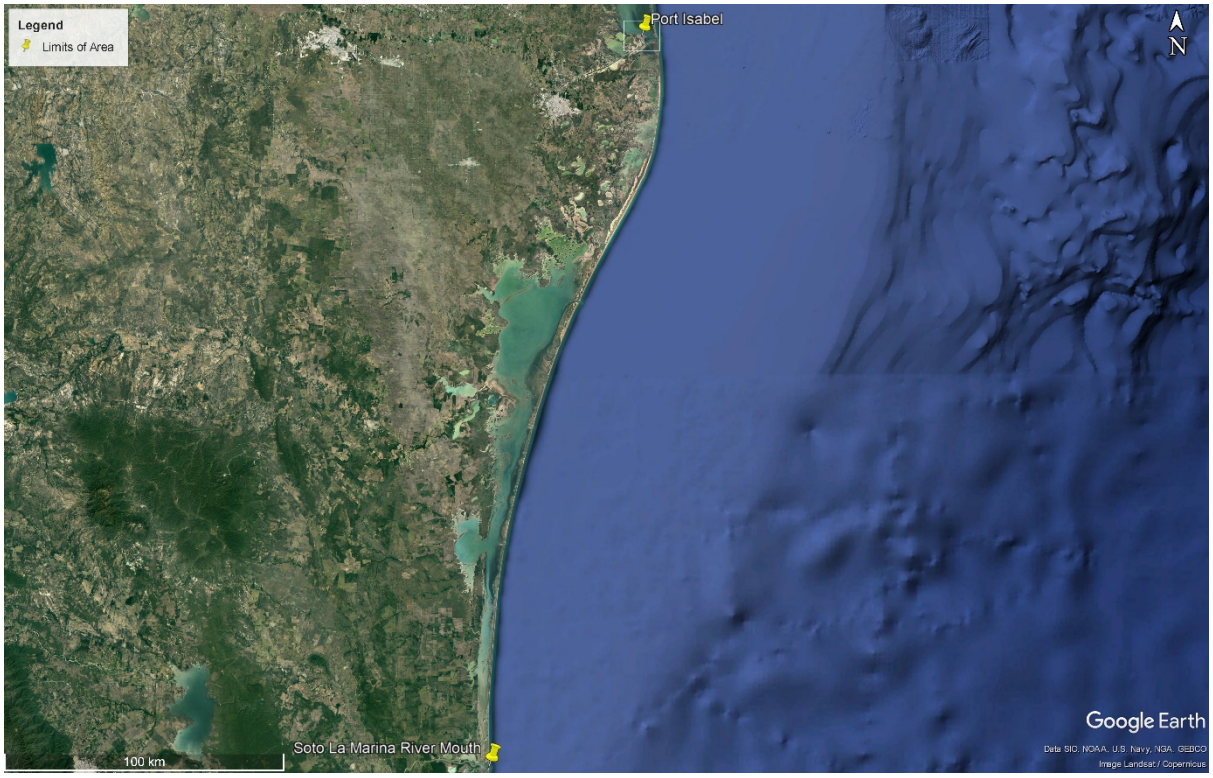


Figure 1: Study area with northern and southern limits

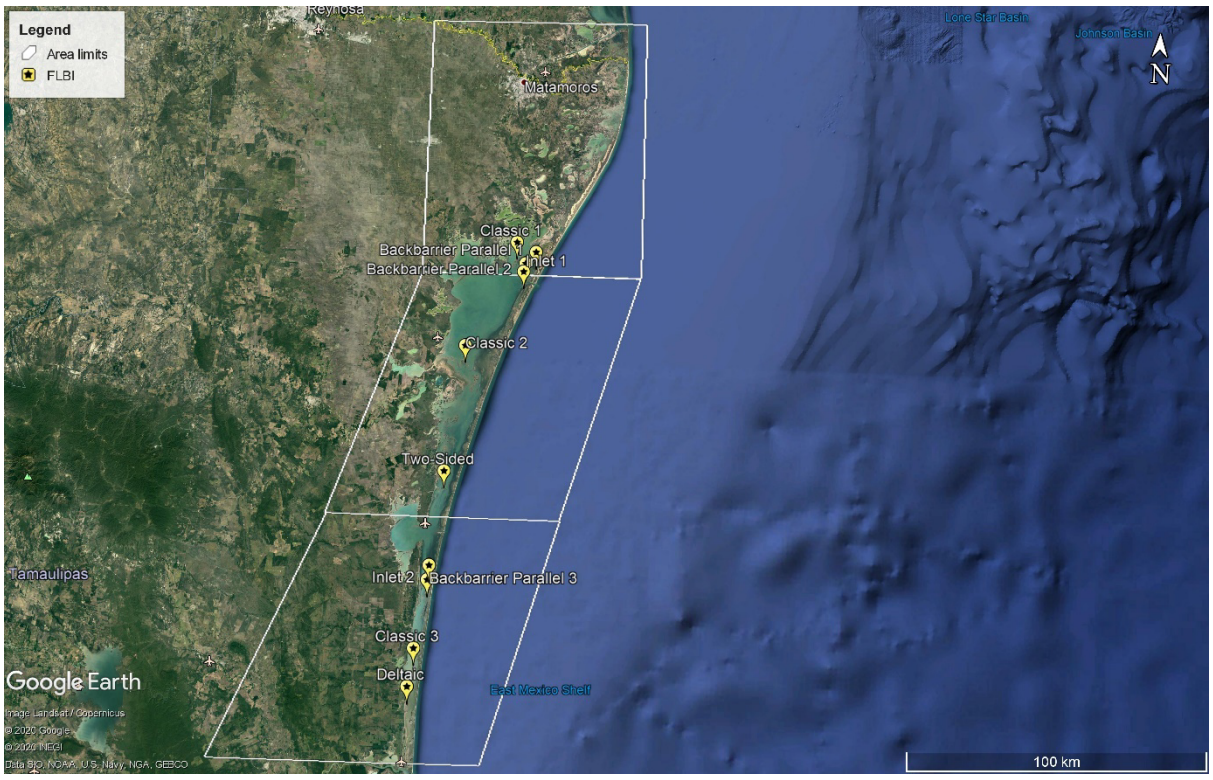


Figure 2: Study area with FLBI locations and subsections

The software package CoastSat was employed to download the individual islands and map their shorelines, using features such as cloud masking and panchromatic image sharpening to provide accurate measurements (Vos et al., 2019). Using CoastSat it is possible to: extract images within generated polygons in Google Earth Engine; map shorelines based upon a range of dates; and specify the satellites used. The date range selected was from 01/01/1984 to 31/12/2019 using the satellites Landsat 5 (L5), Landsat 8 (L8) and Sentinel 2 (S2). Landsat 7 (L7) was excluded due to the error occurring from May 31, 2003 when the Scan Line Corrector (SLC) failed, obscuring some images (USGS.gov, 2020). Shorelines that contained a maximum of 10% cloud cover were then extracted. A reference shoreline (Figure 3) was digitised to limit the area around the island that was considered. Shoreline detections within a predefined distance of this were considered, limiting errors caused by breaches and other anomalies. Shorelines were then selected on a yearly basis provided the image was clear, representative of the general morphology, and between May and September (where possible) for seasonal consistency.

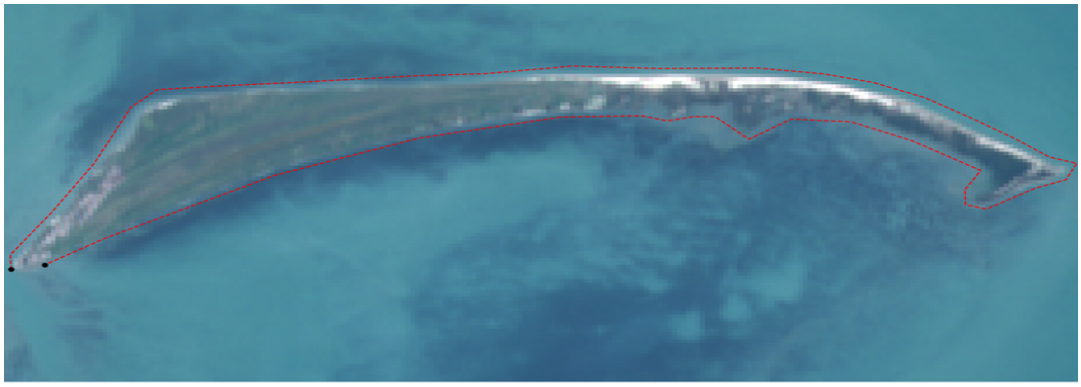

Figure 3: Map of Two-Sided FLBI showing red dashed line as reference shoreline

The extracted shorelines were then exported to QGIS version 3.1 for analysis. Shoreline distance was measured from the oldest shoreline to create a temporal series of positions, along three cross-shore transects (e.g. Figure 3a and 3b). Measurements were taken from the shoreline with the longest fetch (considered the front side), then continued across to the other shoreline (the rear) with the first point of measurement remaining the origin. From this, landward and seaward shoreline positions were determined, allowing a view of yearly change. Tables and graphs were produced to provide a basis to identify patterns and trends in the islands' behaviours, along with a qualitative analysis. Storm data (Figure 5) was gathered from NOAA (National Hurricane Center, 2020) to further aid interpretation by viewing the tracks and severity of tropical storms affecting the Gulf of Mexico.

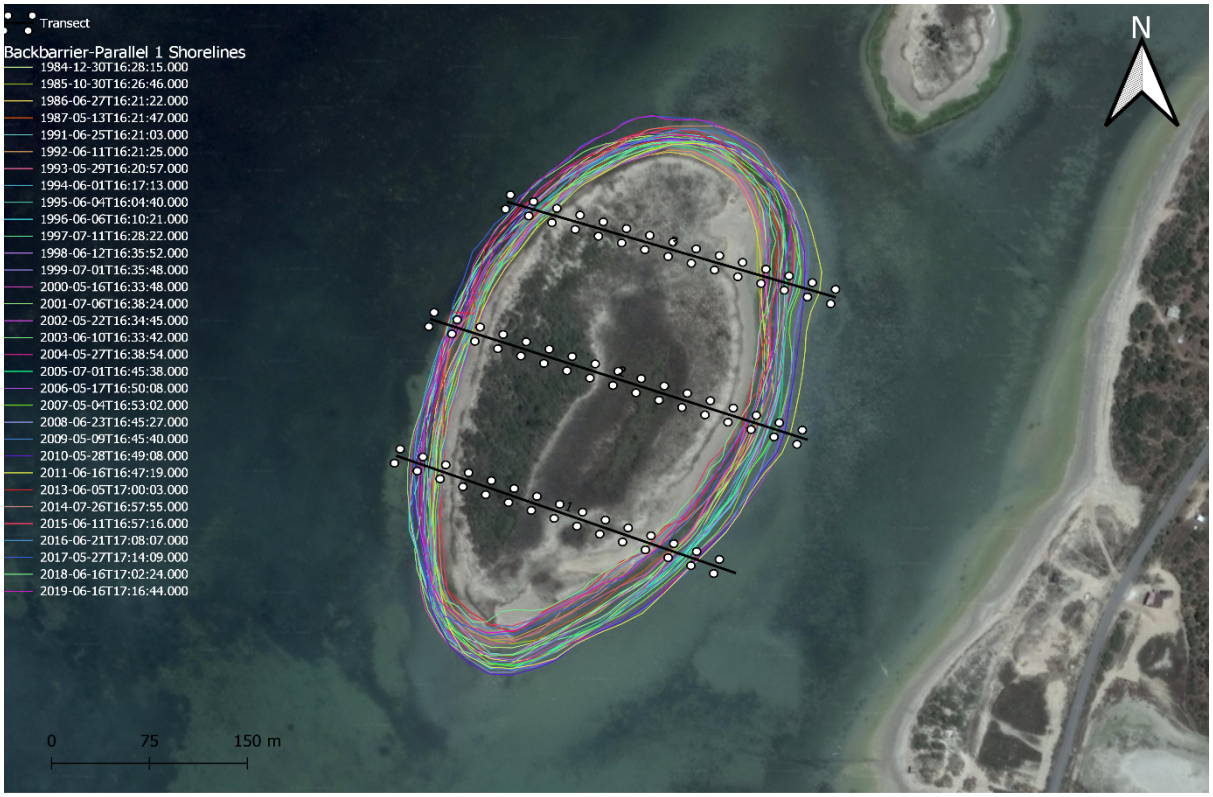


Figure 4a: QGIS output of Backbarrier Parallel 3 with shorelines and transects


Figure 4b: QGIS output of Classic 3 with shorelines and transects

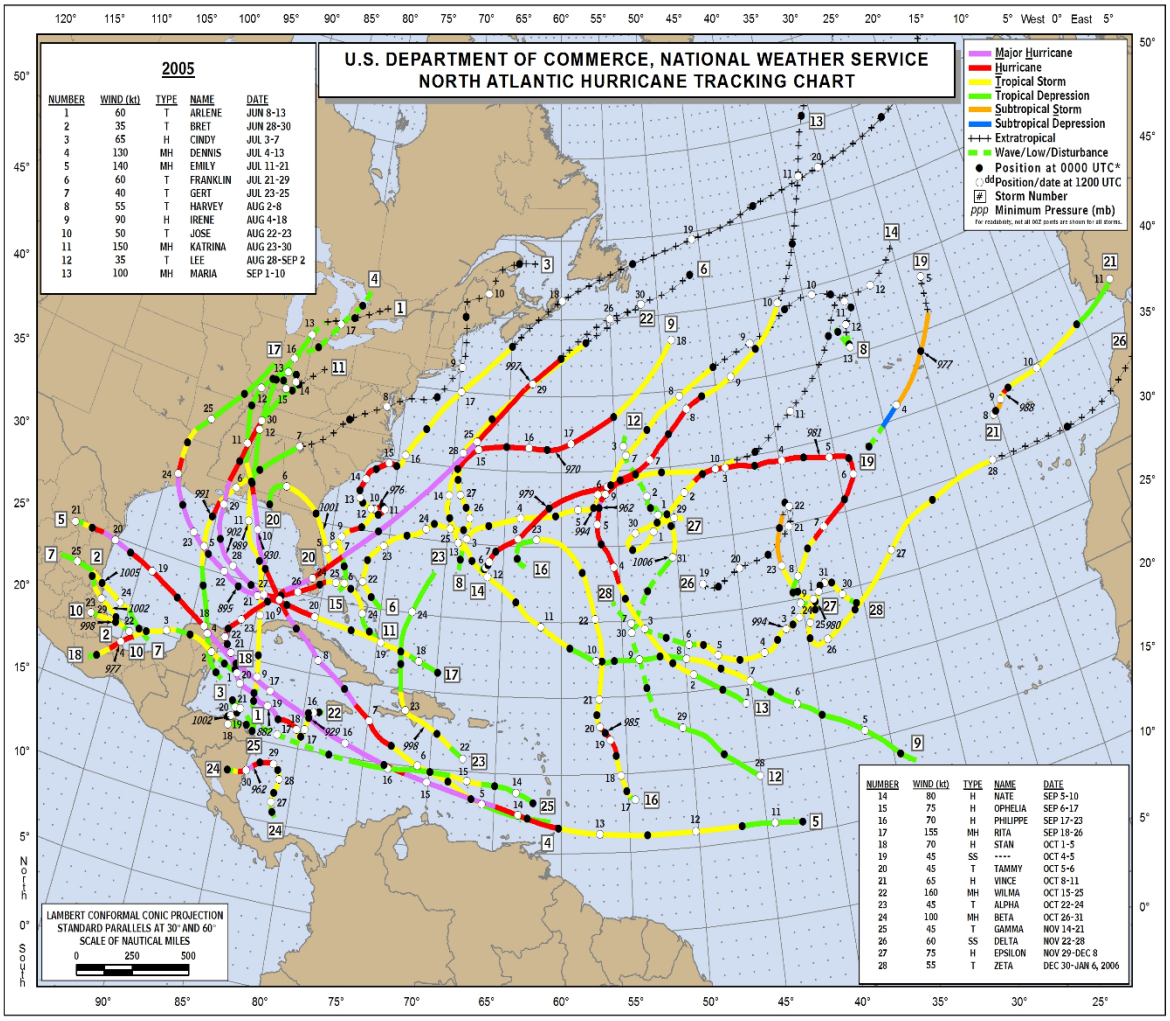


Figure 5: NOAA Atlantic major storm tracks for 2005

## 3. Results

Ten islands were chosen from the three subsections based on the aforementioned criteria (Figure 3). Three Classic FLBIs were identified from all 3 sections, three Backbarrier-parallel (BBP) islands from all sections, two Inlet types from the northern and southern sections, a single Two-Sided island from the central section, and a single Deltaic island from the southern section. Two line graphs were produced for each island, the first representing a time series of shoreline widths as a percentage of the oldest, the second displaying a time series of shoreline migration for both sides of the island.

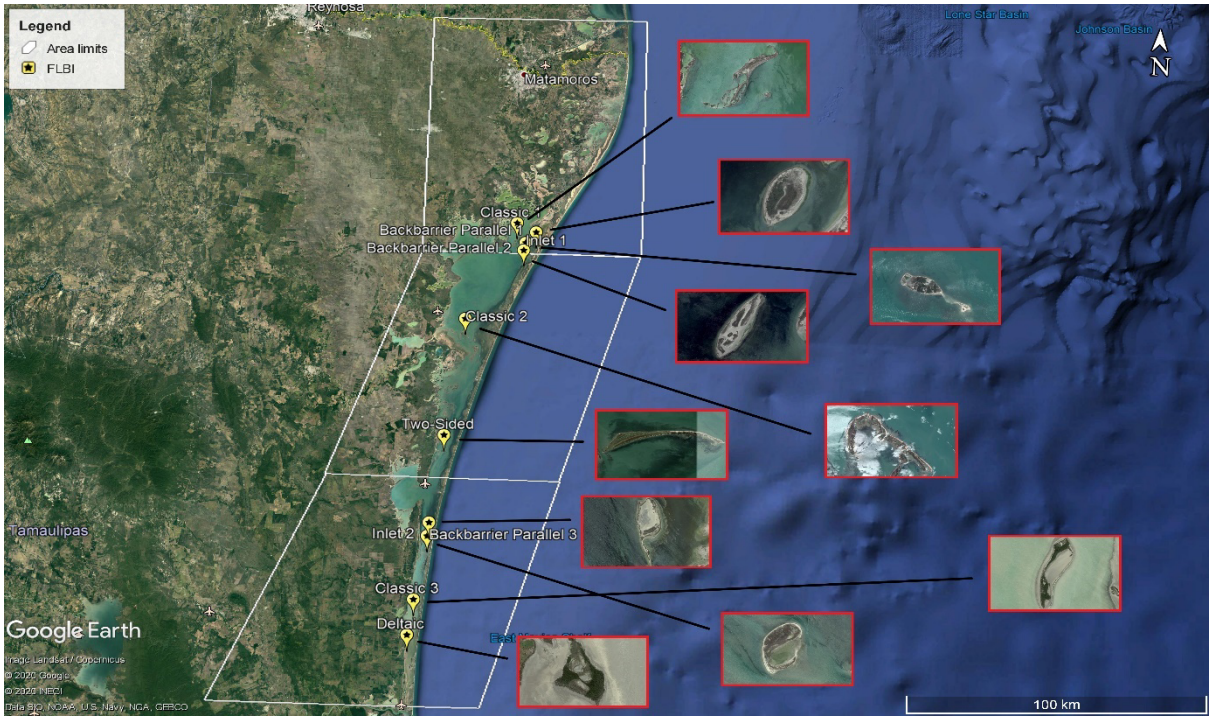


Figure 6: Map of study area with identified FLBI locations

### *3.1.Shoreline Analysis*

All graphs display a yearly series on the x axis. Gaps in data where that year could not be measured show the year only. These gaps were joined in order to produce a visualisation that is easier to interpret. Some observations are missing data from one or more transects due to detection issues, with some continuing general trends but others showing abnormal or skewed data. These however, do not affect the overall quality of the data but are certainly to be considered when interpreting the data.

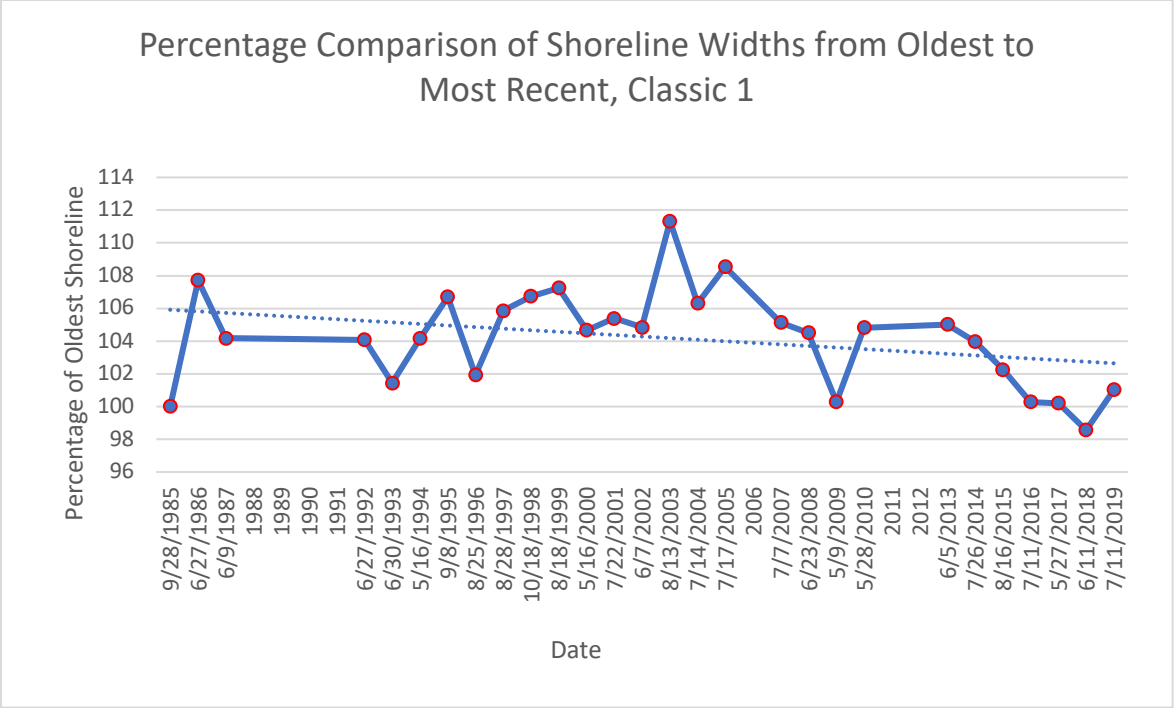


Figure 5a: Graph showing average FLBI widths for Classic 1 based on average of 3 cross-shore transects

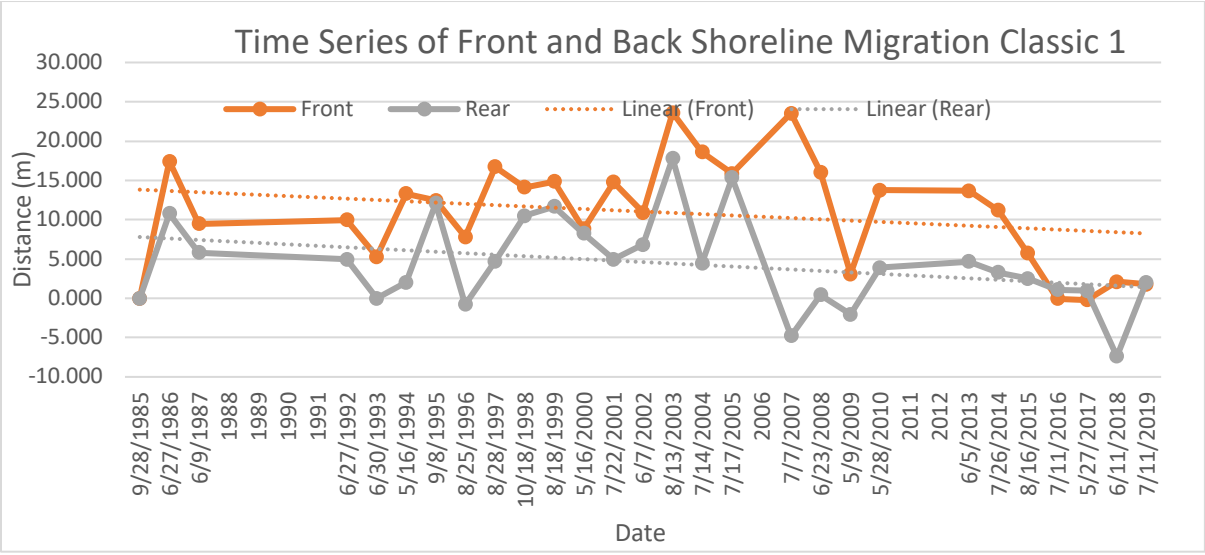


Figure 5b: Graph showing shoreline migration for front and rear sides of Classic 1

Both graphs for Classic 1 display a slight negative trend. Between 2003 and 2008, there is a major gain in island width and shoreline advance on both sides, followed by a sudden, steep fall around 2009. There is a data gap between 1988 and 1991, 2006, 2011 and 2012. Both

graphs show the highest point to be 2003, when the island is at its widest at 110% with the foremost advance in both shorelines. The island is thinnest in 2018, coinciding with the rear shoreline's most significant retreat. The front shoreline that year displayed a slight advance of about 2m. Both shorelines display a similar pattern of change. The start and end dates are relatively similar (at 101% width and a 2m advance). It should be noted that the northern section of the island was isolated for measurement, as the southern section was too unstable (i.e. it regularly disconnected from the northern section) to obtain accurate data.

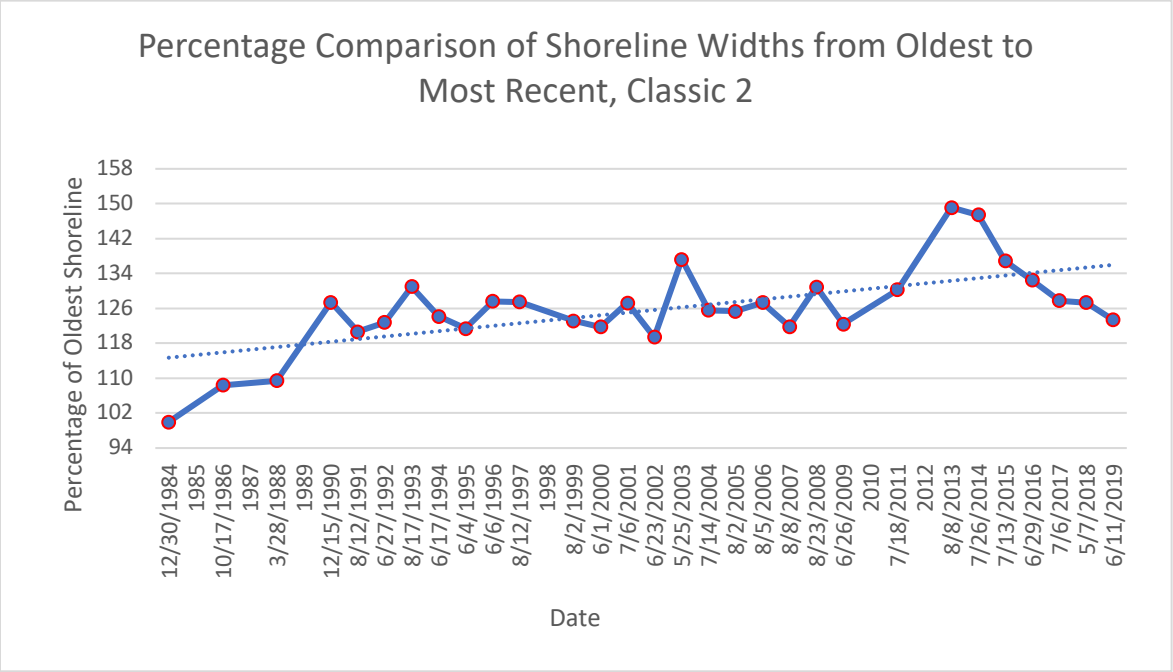


Figure 5c: Graph showing average FLBI widths for Classic 2 based on average of 3 cross-shore transects

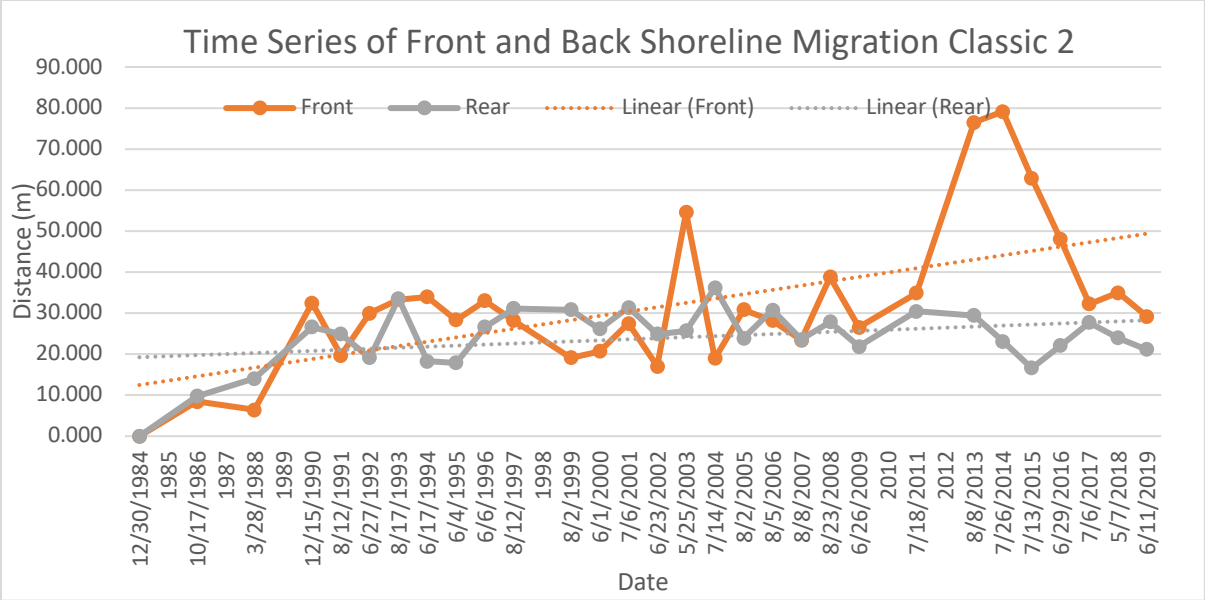


Figure 5d: Graph showing shoreline migration for front and rear sides of Classic 2

Classic 2 displays a data gap for a total of 6 years, 1985, 1987, 1989, 1998, 2010 and 2012. Both graphs show a positive trend overall; however, the trendline for the front side migration shows a significantly greater rise. This is due to elevated measurements in 2003, 2013, and 2014. On these years for transect 2, there was a significant shoreline progradation compared with the other transects. This divergence also displays in the island widths. Its effect is dampened here however, as this graph uses the mean of all 3 transects. The most recent island width shows an increase to 123%. In shoreline migration, the front advances by 29m and the rear by 21m. 1984 represents the island at its thinnest and is also the base point for the shorelines, with all other observations showing an advance. Both shorelines display uniform changes, excluding the two deviations for the front.

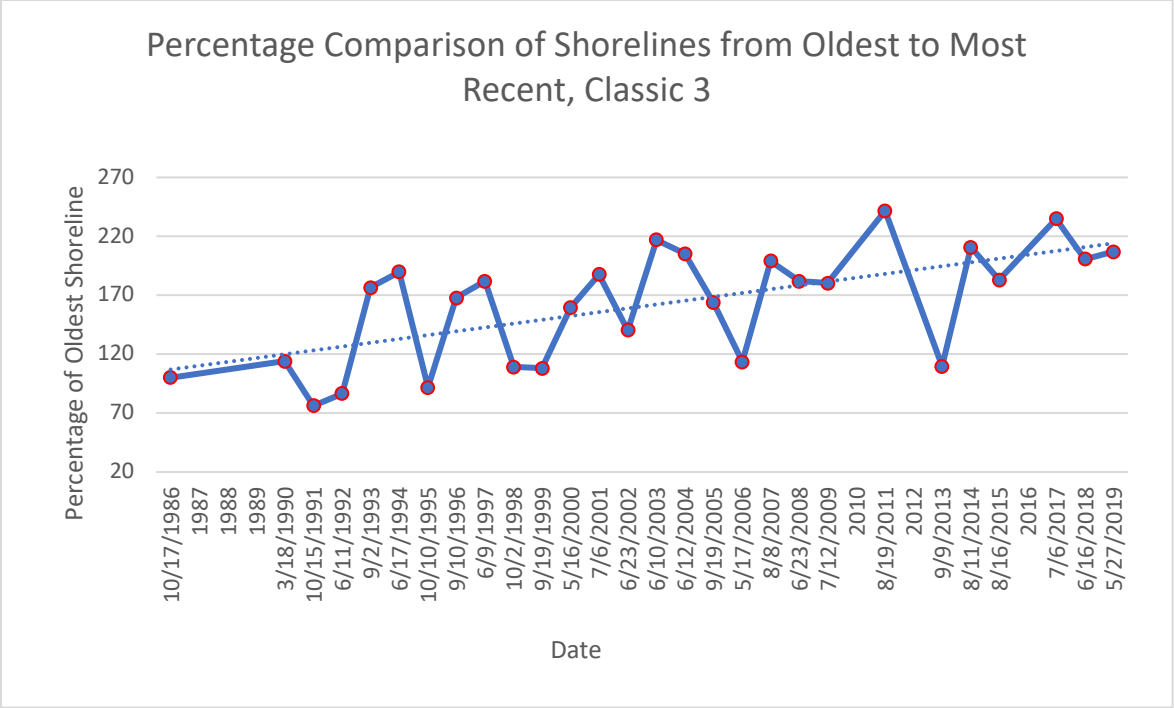


Figure 5e: Graph showing average FLBI widths for Classic 3 based on average of 3 cross-shore transects

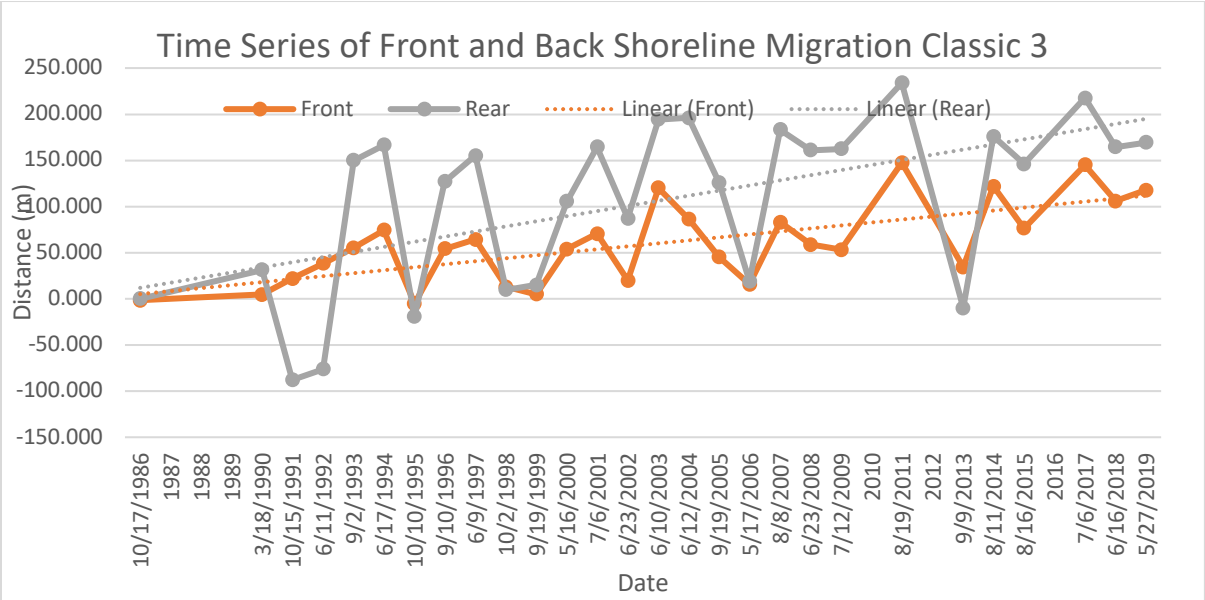


Figure 5f: Graph showing shoreline migration for front and rear sides of Classic 3

Classic 3 shows a positive trend on both graphs. There are data gaps from 1987 to 1989, 2010, 2012 and 2016. The rear measurement for 1985 was excluded as it was based solely

on the 3rd transect, making 1986 a more accurate baseline. Again, this does not greatly affect the accuracy of shoreline widths. Despite the overall positive trend, both graphs show great variability, with significant alternations between rises and falls taking place roughly biennially. Island widths display around a 90% variation between these rises and falls. The two shorelines show a similar pattern of change, with the rear showing slightly more extreme variation. The largest island width falls on 2011 at 242% of the original size, the smallest on 1991 at 76%. The front shoreline's most recent measurement shows an increase of 118m, the rear 169m, from the original.

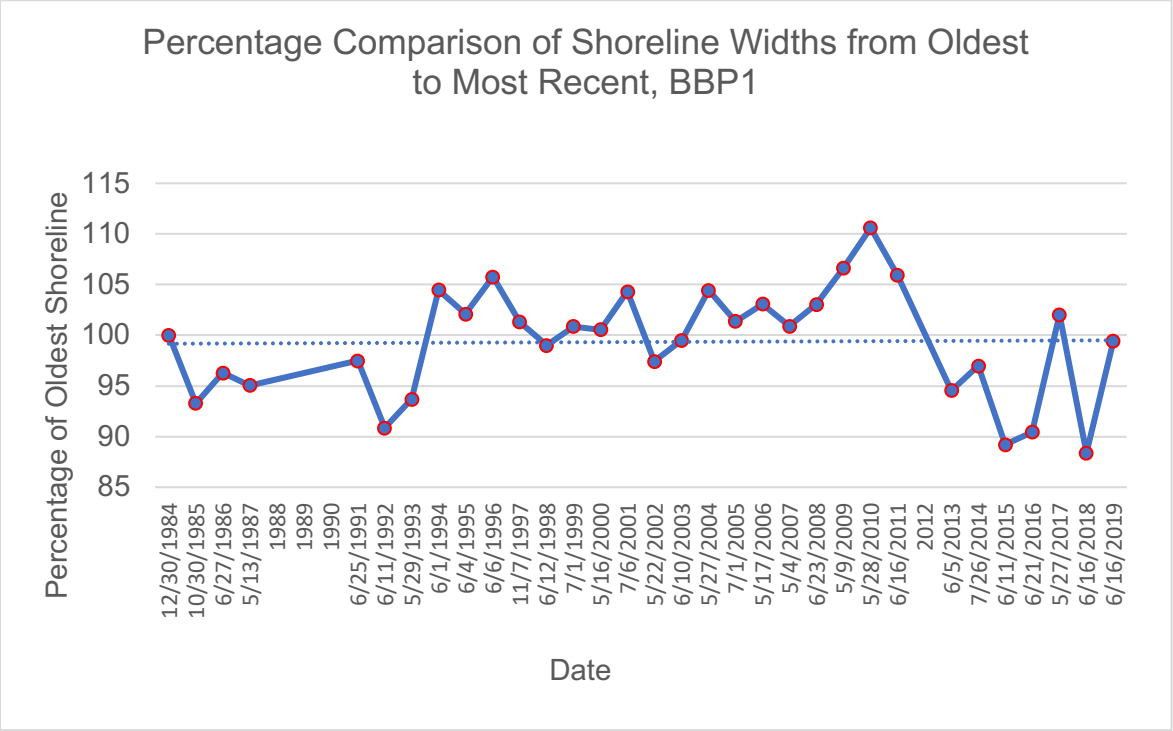


Figure 5g: Graph showing average FLBI widths for Backbarrier Parallel 1 based on average of 3 cross-shore transects

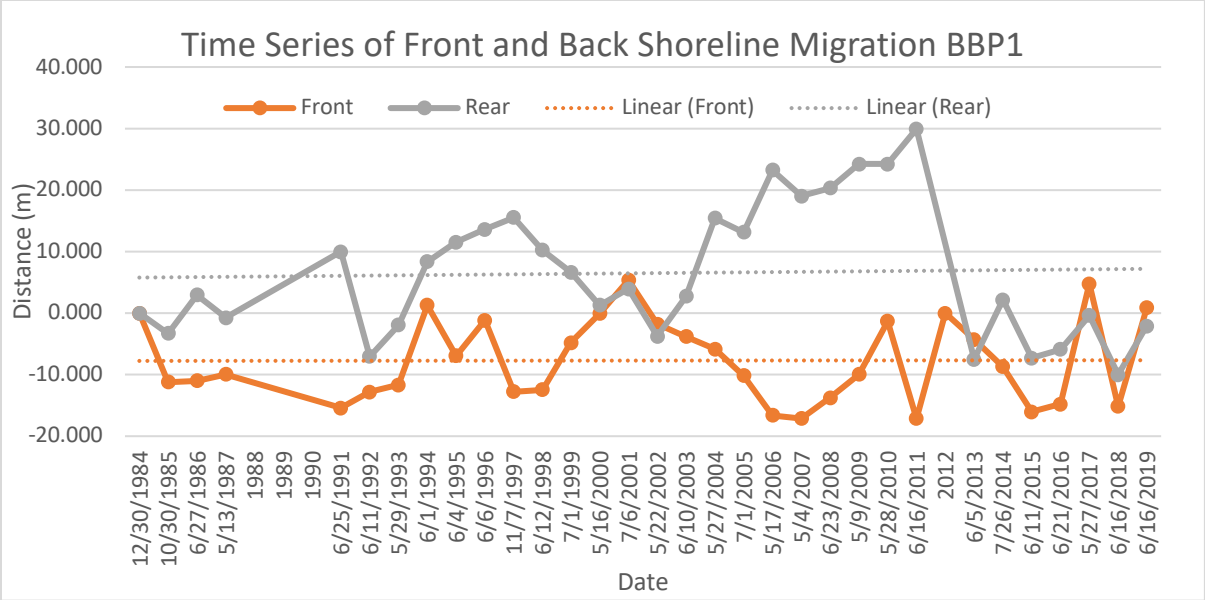


Figure 5h: Graph showing shoreline migration for front and rear sides of Backbarrier Parallel 1

BBP1 shows an even trend on both graphs. Data gaps occur on 1988 to 1990 (2012 for the rear shoreline only). Island widths display a fall to a negative state until around 1992, followed by a rise above 100% to a predominantly positive state until 2011, where it falls again. The two shorelines alternate in pattern, with the rear displaying advance as the front shows retreat, until they begin to correlate in 2017. The shoreline widths are almost identical in 2019, showing a width of 99% compared with 1984. The front shoreline shows a 1m advance from 1984 to 2019 and the rear shows a 2m retreat.

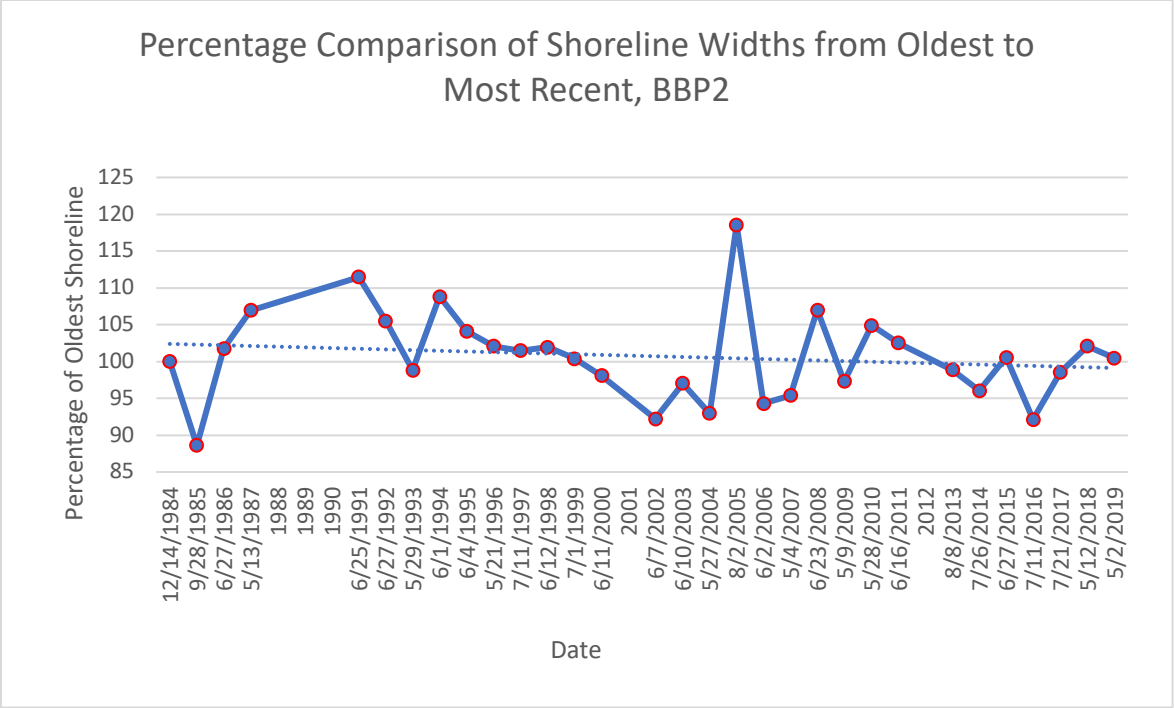


Figure 5i: Graph showing average FLBI widths for Backbarrier Parallel 2 based on average of 3 cross-shore transects

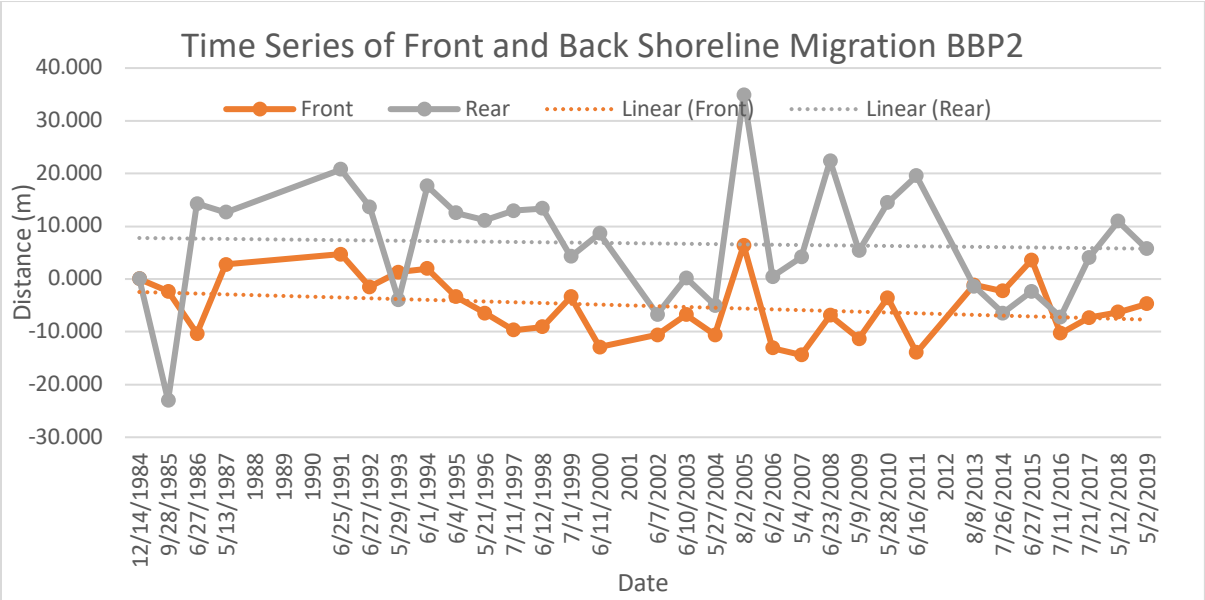


Figure 5j: Graph showing shoreline migration for front and rear sides of Backbarrier Parallel 2

BBP2 displays a slight negative trend on both graphs. Data gaps exist for 1988 to 1990, 2001 and 2012. There is a significant rise in width (26%,). From 2004 to 2005, the shorelines show a 16m advance from the front and a 30m advance for the rear, followed by a sharp drop in 2006. Both shorelines display a similar pattern of change, with the rear displaying the majority of advance excluding 3 occasions, where it temporarily falls below the frontal growth, around 1995, 1983 and 2014. The island width returns to an identical size as the first observation in 2014, despite the final shoreline measurements showing positive for the rear and negative for the front.

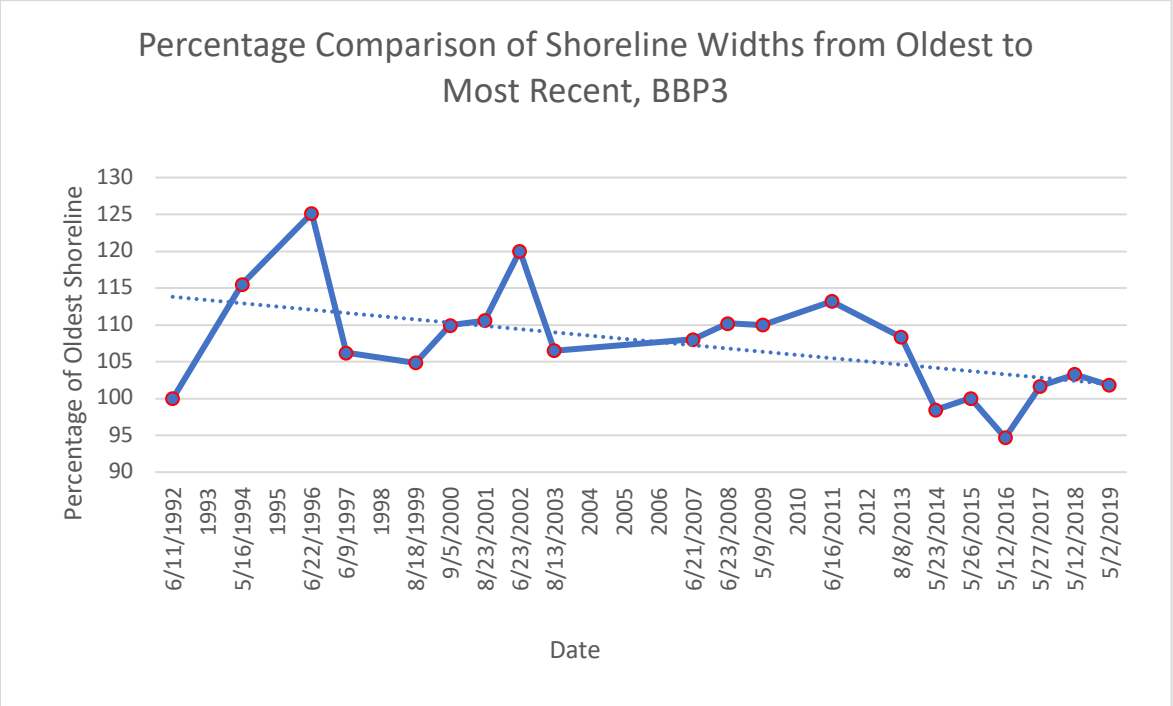


Figure 5k: Graph showing average FLBI widths for Backbarrier Parallel 3 based on average of 3 cross-shore transects

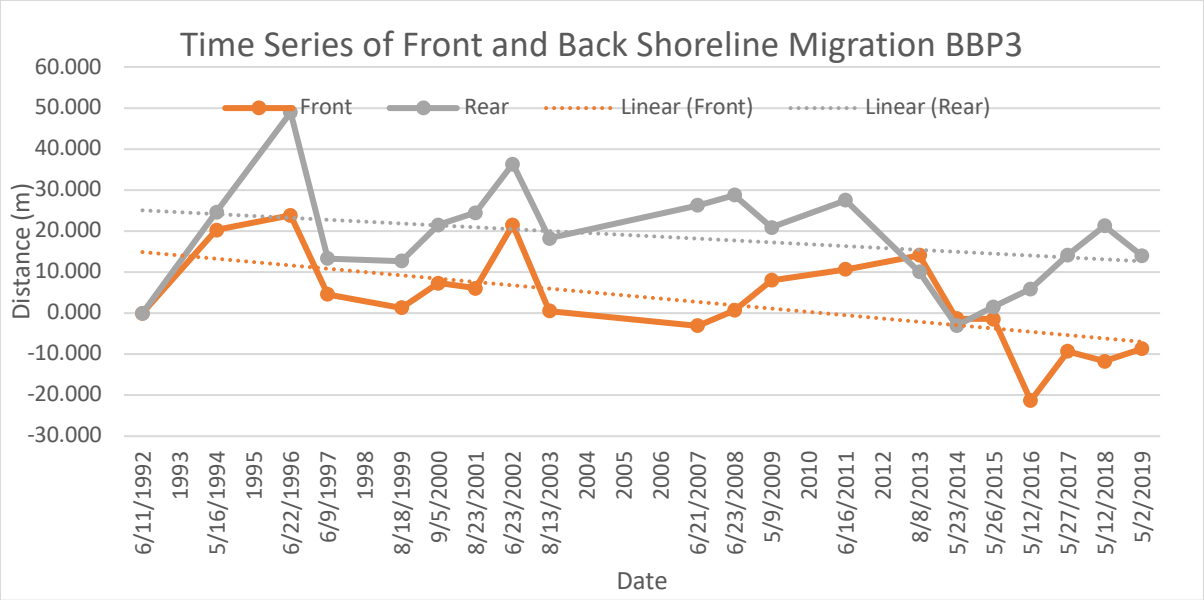


Figure 5l: Graph showing shoreline migration for front and rear sides of Backbarrier Parallel 3

BBP3 shows a negative trend on both graphs, with the frontal shoreline showing slightly more retreat. Observations begin in 1992 as prior images were not available in enough detail to successfully identify the shorelines. 8 years lack data, 1993, 1995, 1998, 2004 to 2006, 2010 and 2012. Island widths show four distinct events of significant rise then fall along the steady overall decline. This is also reflected in both shorelines, with the front slightly deviating from 2015 to 2016. Despite the negative trend, the islands width measures 102% of the original in 2019. This could be due to the extreme rise in 1996 (the highest point with 125% width, a 24m advance on the front shoreline, and a 49m advance on the rear), skewing the data slightly. Similar to BBP2, the island's shoreline series terminates with a similar width to the first measurement, despite the front shoreline having retreated and the rear having advanced.

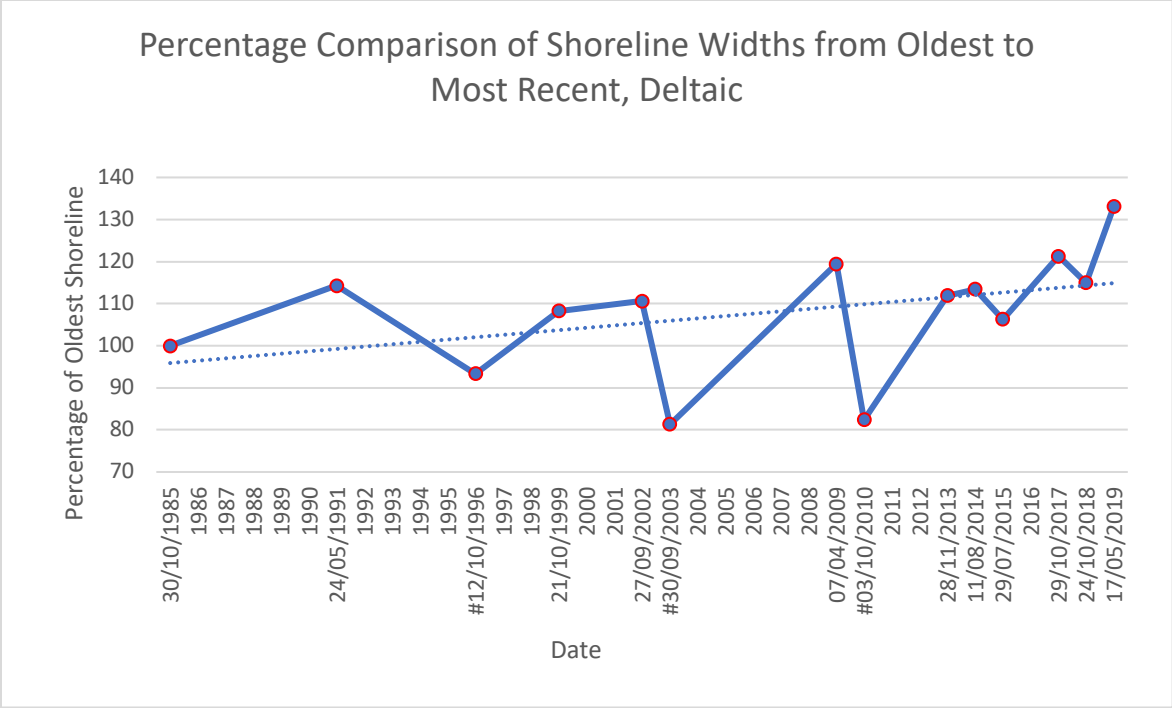


Figure 5m: Graph showing average FLBI widths for Deltaic based on average of 3 cross-shore transects

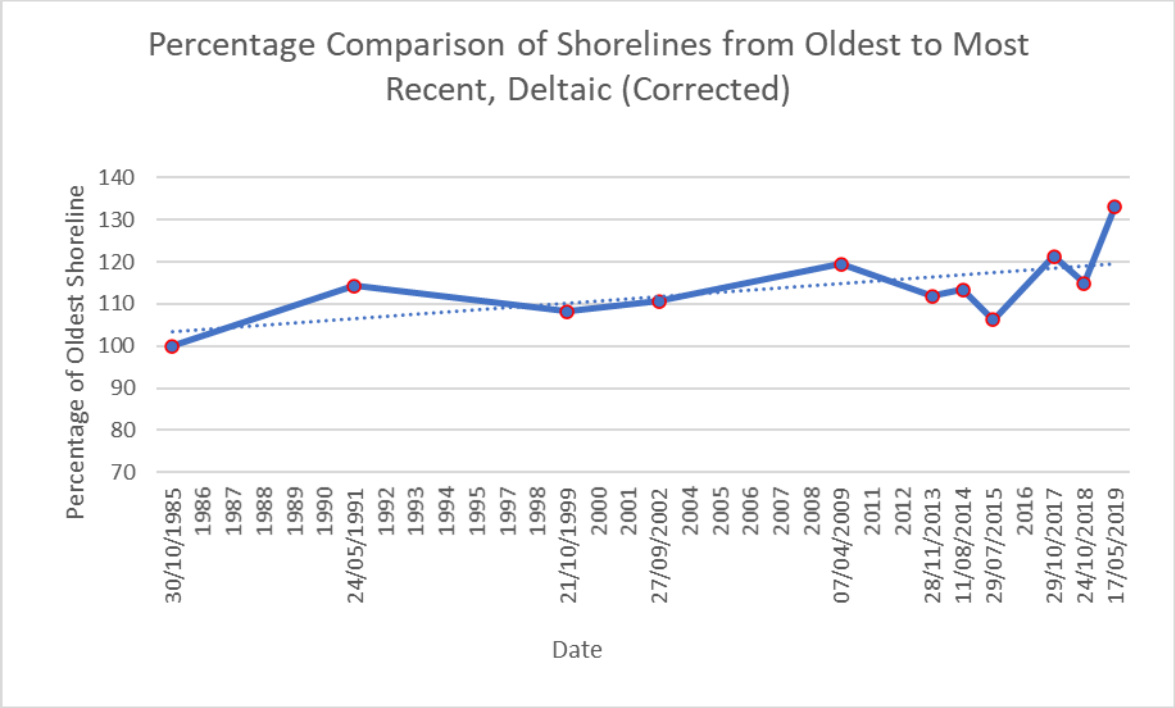


Figure 5m1: Graph showing average FLBI widths for Deltaic based on average of 3 cross-shore transects excluding measurements for 1996, 2003 and 2010

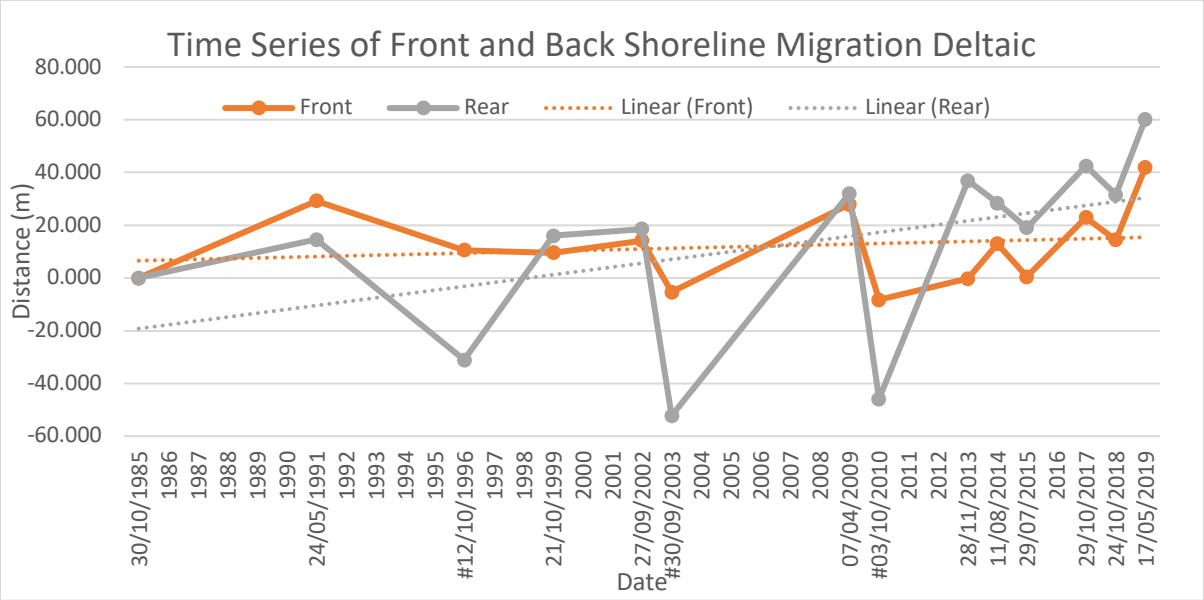


Figure 5n: Graph showing shoreline migration for front and rear sides of Deltaic

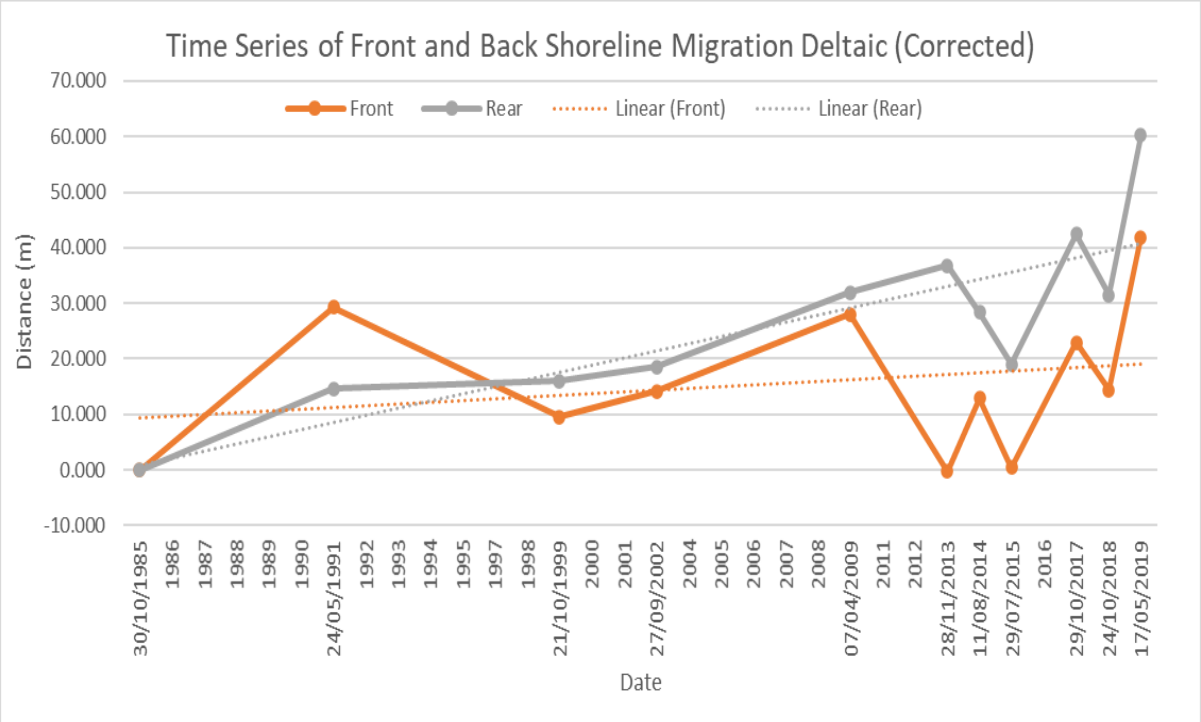


Figure 5n1: Graph showing shoreline migration for front and rear sides of Deltaic excluding measurements for 1996, 2003 and 2010

For the Deltaic FLBI, measurements for transect 2 are absent from 1996, 2003 and 2010. Corrected graphs are displayed to compare measurements with those years excluded. These graphs show similar trendlines suggesting that these dates do not have a significant affect on the overall trends. There are a total of 21 missing dates. All graphs show a positive trend, with

the rear shoreline advancing more consistently than the front. The shorelines display a similar pattern of change, more evident toward the more recent dates. The 2019 width measurement shows an increase to 133% from 1985, the rear shoreline shows advance by 60m, and the front by 42m. These measurements are also the highest recorded.

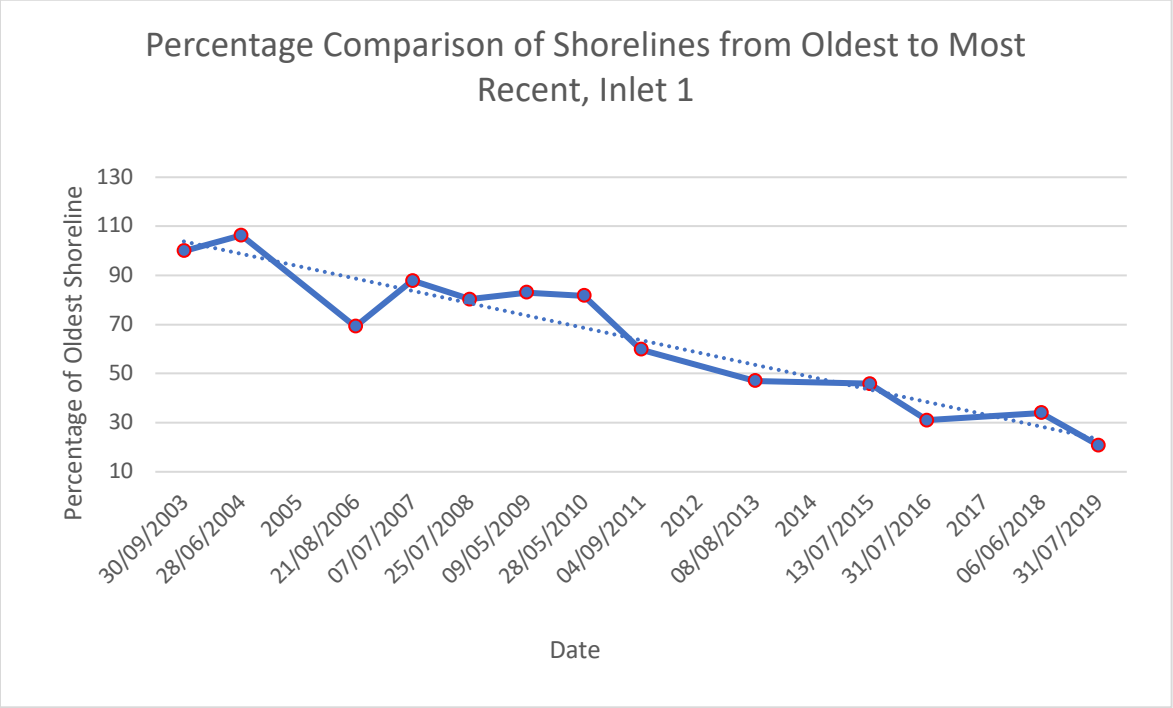


Figure 5o: Graph showing average FLBI widths for Inlet 1 based on average of 3 cross-shore transects

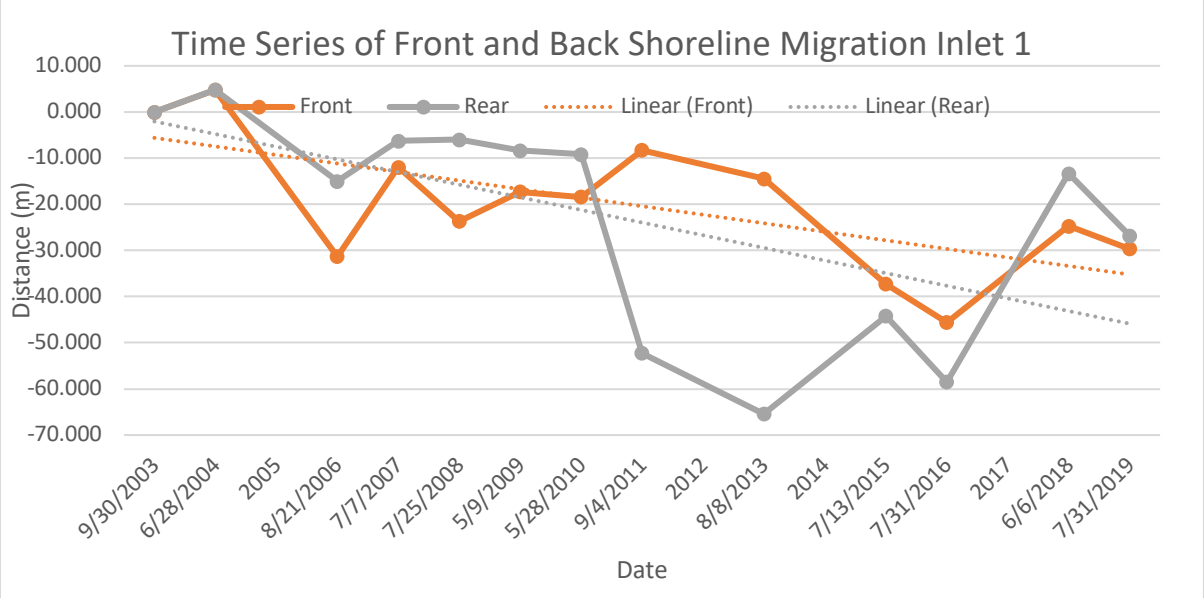

Figure 5p: Graph showing shoreline migration for front and rear sides of Inlet 1

Inlet 1 has gaps in data for 2005, 2012, 2014, and 2017. Measurements for transect 3 are absent from 2011, 2013, 2016, and 2019. Transect 1 measurements are absent from 2018 and 2019. Both graphs display a negative trend, with the rear shoreline showing greater retreat, as well as a major fall from 2011 to 2013 (around a 55m retreat). This fall could be a product of missing transect data however, with the mean widths representing a more accurate view. This island shows a major decline at only 21% of its original width in 2019, with the shorelines retreating by 27m (rear) and 30m (front). The island experienced its maximum width in 2004 at 106%, as well as roughly a 5m shoreline advance on both sides.

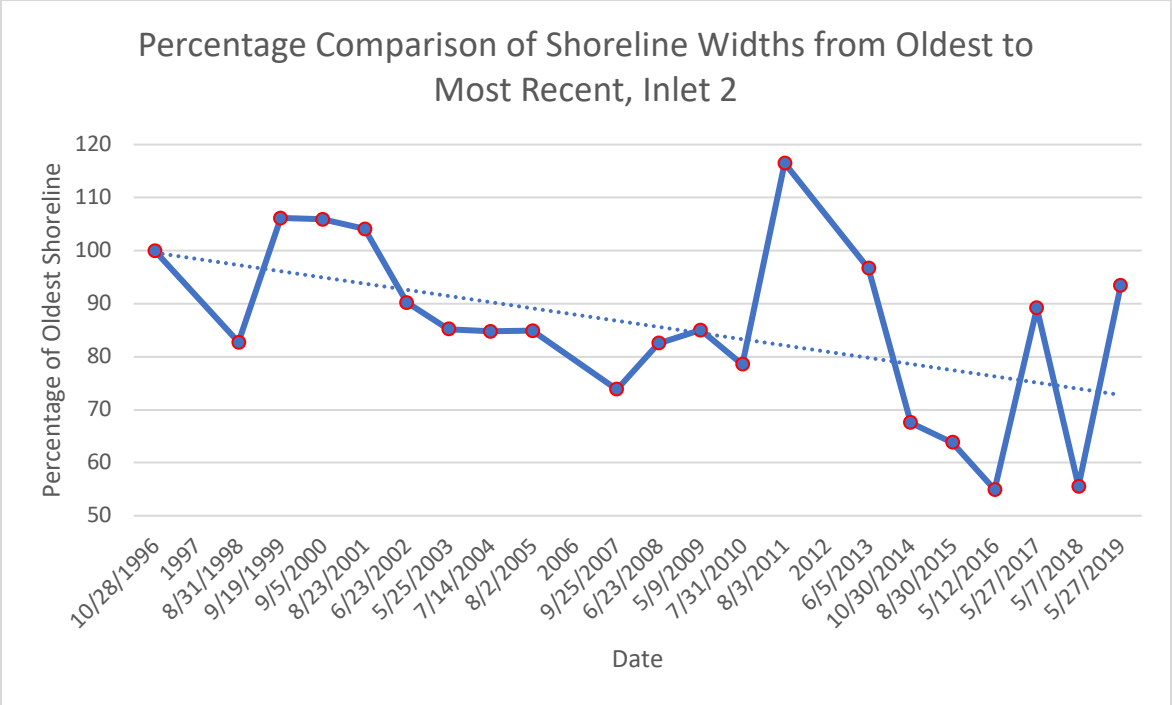


Figure 5q: Graph showing average FLBI widths for Inlet 2 based on average of 3 cross-shore transects

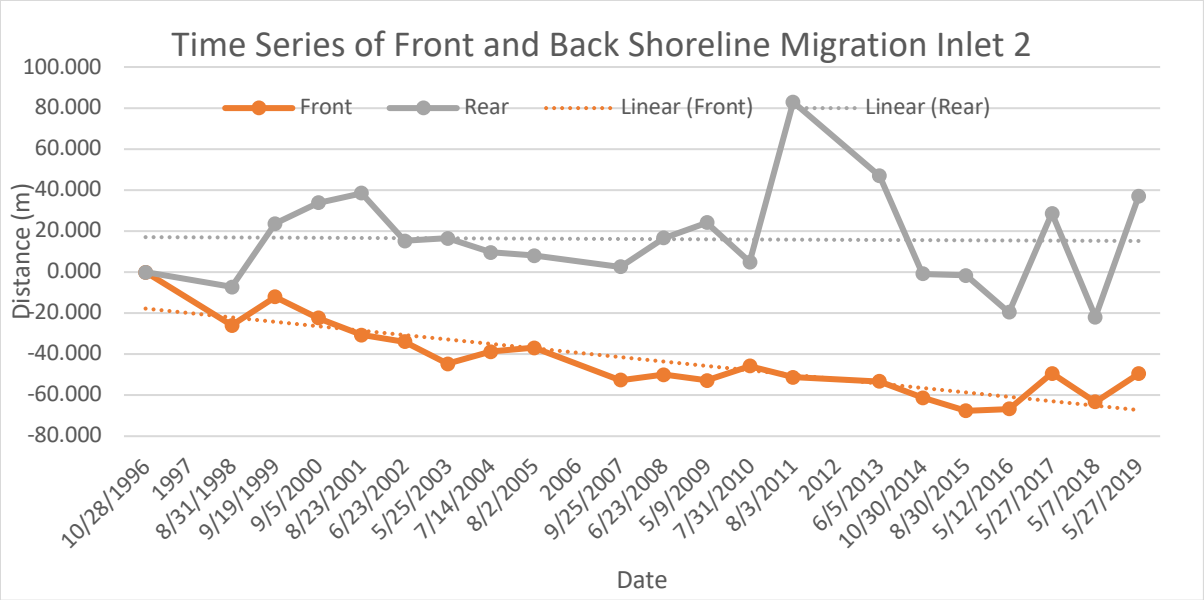


Figure 5r: Graph showing shoreline migration for front and rear sides of Inlet 2

Inlet 2 displays a negative trend on both graphs; however, the front shoreline shows a greater decline than the rear. This could be due to a large rear advance from 2010 to 2011, where the shoreline reaches a maximum of 83m. 2011 also represents the maximum width at 117% of its original size. Measurements were taken from 1996 due to the island only forming around then, thus allowing the first measurements to be taken. There are data gaps for 1997, 2006 and 2012. 2019 displays a close percentage to 1996 in terms of island width at 93% of its original size, though the rear shoreline shows an advance up to 37m and the front a retreat falling to -50m in 2019. This would suggest the island is migrating toward its rear side.

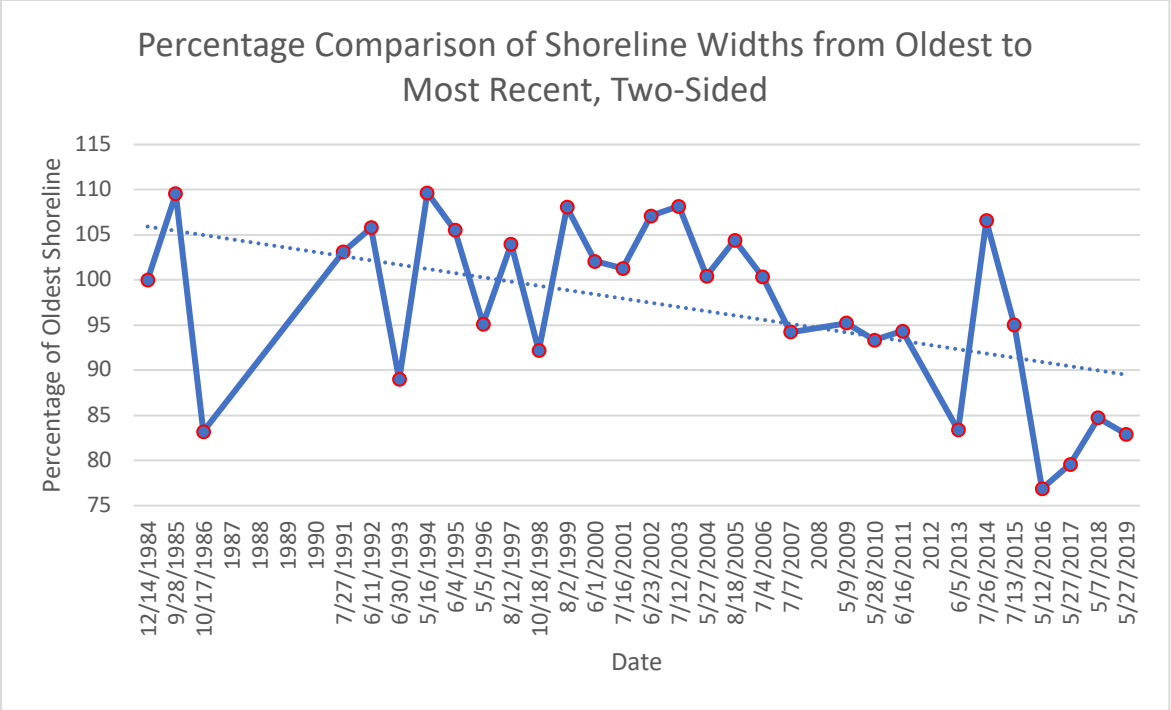


Figure 5s: Graph showing average FLBI widths for Two-Sided based on average of 3 cross-shore transects

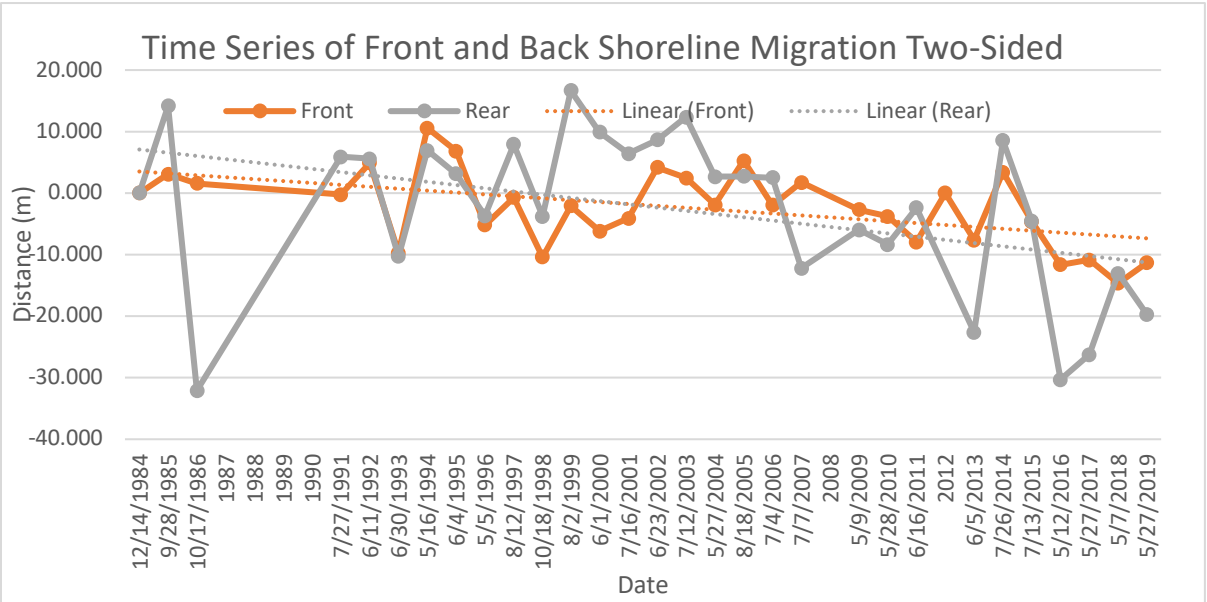


Figure 5t: Graph showing shoreline migration for front and rear sides of Two-Sided

The Two-Sided FLBI displays a negative trend on both graphs. Data is absent for 1987 to 1990, 2008 and 2012. 1986 lacks a measurement for transect 3, possibly skewing the data

and causing the large fall observed that year. Although the two shorelines show a similar pattern of change, they regularly invert in terms of advance/retreat, with the rear shoreline showing a slightly greater negative trend overall. The island width for 2019 is 83% of the original measurement, with the rear shoreline retreating by 20m and the front by 11m.

### *3.2. Statistical Analysis*

Table 1: Descriptive analysis of FLBI migration showing number of observations, range, minimum and maximum, mean statistic and standard error, and standard deviations

| | N | Range | Minimum | Maximum | Mean | | Std. Deviation |
|---|---|---|---|---|---|---|---|
| | | | | | Statistic | Std. Error | |
| Classic 1 Average distance from oldest shoreline (Front) | 28 | 23.84 | -.23 | 23.62 | 10.8750 | 1.27624 | 6.75322 |
| Classic 1 Average Distance From Oldest Shoreline (Rear) | 28 | 25.21 | -7.40 | 17.81 | 4.4266 | 1.09010 | 5.76825 |
| Classic 2 Average distance from oldest shoreline (Front) | 30 | 79.14 | .00 | 79.14 | 31.9053 | 3.25976 | 17.85446 |
| Classic 2 Average Distance From Oldest Shoreline (Rear) | 30 | 36.18 | .00 | 36.18 | 23.9858 | 1.35822 | 7.43929 |
| Classic 3 Average distance from oldest shoreline (Front) | 28 | 152.50 | -5.14 | 147.36 | 59.9479 | 8.33400 | 44.09941 |
| Classic 3 Average Distance From Oldest Shoreline (Rear) | 28 | 321.77 | -87.91 | 233.86 | 102.3256 | 17.05422 | 91.83980 |
| BBP1 Average distance from oldest shoreline (Front) | 33 | 22.51 | -17.13 | 5.37 | -7.7078 | 1.18153 | 6.78738 |
| BBP1 Average Distance From Oldest Shoreline (Rear) | 32 | 39.93 | -9.99 | 29.94 | 6.5213 | 1.92679 | 10.89955 |
| BBP2 Average distance from oldest shoreline (Front) | 31 | 20.82 | -14.40 | 6.42 | -5.2094 | 1.05312 | 5.86355 |
| BBP2 Average Distance From Oldest Shoreline (Rear) | 31 | 57.86 | -23.02 | 34.84 | 6.7143 | 2.03799 | 11.34705 |
| BBP3 Average distance from oldest shoreline (Front) | 20 | 45.19 | -21.34 | 23.85 | 3.0985 | 2.56923 | 11.48994 |
| BBP3 Average Distance From Oldest Shoreline (Rear) | 20 | 51.98 | -3.06 | 48.92 | 18.3765 | 2.81508 | 12.58944 |
| Deltaic Average distance from oldest shoreline (Front) | 14 | 50.10 | -8.26 | 41.84 | 12.1559 | 3.86646 | 14.46697 |
| Deltaic Average Distance from Oldest Shoreline (Rear) | 14 | 112.52 | -52.27 | 60.25 | 12.1587 | 8.93067 | 33.41553 |
| Inlet 1 Average distance from oldest shoreline (Front) | 13 | 50.37 | -45.60 | 4.77 | -19.8364 | 3.97679 | 14.33851 |
| Inlet 1 Average Distance from Oldest Shoreline (Rear) | 13 | 70.22 | -65.43 | 4.79 | -23.1140 | 6.60928 | 23.83009 |
| Inlet 2 Average distance from oldest shoreline (Front) | 21 | 67.64 | -67.64 | .00 | -43.2914 | 3.85047 | 17.64507 |
| Inlet 2 Average Distance from Oldest Shoreline (Rear) | 21 | 104.76 | -21.87 | 82.89 | 16.0874 | 5.22702 | 23.95320 |
| Two-Sided Average distance from oldest shoreline (Front) | 31 | 25.24 | -14.66 | 10.58 | -2.3721 | 1.10948 | 6.17735 |
| Two-Sided Average Distance from Oldest Shoreline (Rear) | 30 | 48.73 | -32.08 | 16.65 | -2.7002 | 2.40331 | 13.16346 |

Table 2: Descriptive analysis of FLBI widths showing number of observations, range, minimum and maximum, mean statistic and standard error, and standard deviations

| | N | Range | Minimum | Maximum | Mean | | Std. Deviation |
|---|---|---|---|---|---|---|---|
| | | | | | Statistic | Std. Error | |
| Classic 1 Average Island Width | 28 | 46.70 | 360.33 | 407.03 | 380.9071 | 2.05187 | 10.85746 |
| Classic 1 % of Oldest Shoreline | 28 | 12.77 | 98.56 | 111.33 | 104.1853 | .56122 | 2.96967 |
| Classic 2 Average Island Width | 30 | 105.96 | 215.65 | 321.61 | 271.5407 | 3.86312 | 21.15916 |
| Classic 2 % of Oldest Shoreline | 30 | 49.13 | 100.00 | 149.14 | 125.9176 | 1.79139 | 9.81182 |
| Classic 3 Average Island Width | 28 | 447.37 | 206.02 | 653.39 | 438.1070 | 24.57940 | 130.06197 |
| Classic 3 % of Oldest Shoreline | 28 | 166.00 | 76.00 | 242.00 | 162.1429 | 9.09019 | 48.10075 |
| BBP1 Average Island Width | 32 | 48.05 | 191.05 | 239.10 | 214.7549 | 2.06570 | 11.68539 |
| BBP1 % of Oldest Shoreline | 32 | 22.22 | 88.38 | 110.60 | 99.3398 | .95553 | 5.40532 |
| BBP2 Average Island Width | 31 | 66.61 | 196.99 | 263.60 | 223.8435 | 2.44884 | 13.63456 |
| BBP2 % of Oldest Shoreline | 31 | 29.96 | 88.60 | 118.56 | 100.6769 | 1.10140 | 6.13232 |
| BBP3 Average Island Width | 20 | 88.19 | 273.88 | 362.07 | 310.7801 | 4.79980 | 21.46534 |
| BBP3 % of Oldest Shoreline | 20 | 30.48 | 94.67 | 125.15 | 107.4230 | 1.65908 | 7.41963 |
| Deltaic Average Island Width | 14 | 159.66 | 250.19 | 409.85 | 332.0824 | 11.91896 | 44.59665 |
| Deltaic % of Oldest Shoreline | 14 | 51.88 | 81.29 | 133.17 | 107.9004 | 3.87274 | 14.49045 |
| Inlet 1 Average Island Width | 13 | 128.85 | 31.44 | 160.29 | 98.2205 | 11.51145 | 41.50512 |
| Inlet 1 % of Oldest Shoreline | 13 | 85.49 | 20.86 | 106.34 | 65.1637 | 7.63717 | 27.53622 |
| Inlet 2 Average Island Width | 21 | 117.83 | 105.12 | 222.96 | 164.1684 | 6.86510 | 31.45982 |
| Inlet 2 % of Oldest Shoreline | 21 | 61.57 | 54.93 | 116.50 | 85.7848 | 3.58727 | 16.43894 |
| Two-Sided Average Island Width | 30 | 59.50 | 139.58 | 199.08 | 176.3863 | 3.18787 | 17.46066 |
| Two-Sided % of Oldest Shoreline | 30 | 32.78 | 76.89 | 109.66 | 97.1623 | 1.75603 | 9.61816 |

Classic 3 shows the largest standard deviation in terms of both shorelines and overall width, as well as the largest standard error of the mean. It also has the largest range of measurements for both shorelines (152.5m front, 321.77m rear), the average island widths (447.37m), and percentage widths (96.93%), displaying great variability. Classic 1 shows the smallest standard deviation for percentage widths at 2.96, as well as the lowest for average widths at 10.85. At 5.76, it also displays the lowest standard deviation for the rear shoreline. BBP2 shows the lowest standard deviation for the front shoreline at 5.86. Again, Classic 1 shows the lowest standard error of the mean for the rear shoreline at 1.09, percentage shoreline widths at 0.56, and average widths at 2.05. BBP2 shows the lowest measurement for the front shoreline at 1.05. Classic 1 has the smallest range of measurements for both average island width (46.7m) and percentage (12.77%), as well as the rear shoreline (25.21m). BBP2 has the smallest range for the front shoreline (20.82m).

## 4. Discussion

### *4.1. Design and Limitations*

Shorelines were examined on a yearly basis, as sampling less provided an inadequate number of observations required for an accurate interpretation, and more than once a year resulted in several issues. The chief among these was that shorelines would be too clustered to make observations through excess 'noise' from false detections. These occurred when CoastSat included breaches or other landforms in the digitised shoreline, attempting to create a path to them. Reference shorelines were used within CoastSat to reduce these false detections. Their use was limited however, as the islands with a more complex geomorphological progression could 'outgrow' the reference, resulting in a lack of detection at later dates and for more extreme advances or declines.

### *4.2. Quantitative Analysis*

Classic 1 displays a strong correlation for both shorelines and returns to roughly its original width on four separate years. Both shorelines for 2019 show the same slight accretion, suggesting that the island is in a stable state, rarely dropping below 1985 levels. This is supported by the low standard deviation for the shoreline and width measurements, as well as the low standard error. The sudden rise in 1986, maintained until 2009, and subsequent steady decline from 2013, are responsible for the trendlines being negative despite the numerous positive observations. This suggests that the sediment supply available is plentiful and mobile, probably through storm driven transport (Cooper, Lewis and Pilkey, 2007), and/or the original measurement was taken on a low year in terms of shoreline width. With relatively little or no change to island width in 2019 compared to 1985, along with both shorelines showing similar migration, it suggests that the island is active but not migrating.

Classic 2 displays a strong positive trend, with a steady rise in both shorelines and the island width. It is possible that the island is still evolving, while also beginning to settle into a stable state. Unlike Classic 1, the observations for both width and shoreline migration never drop below 1984 levels, reinforcing the conclusion that the island is actively developing. The significant advance in the front shoreline for the three years at transect 2 appears to be natural, and is probably the product of excess sediment being supplied to that area of the island. As they occur on 2003 and then ten years later on 2013, they are probably caused by a specific type of event. It is possible that Hurricane Ingrid in 2013 could have been a major influence, increasing sediment transport greatly. In 2003 however, there is no hurricane preceding this

advance (Hurricane Erika made landfall after the observation date), leading to the conclusion that it is probably part of a natural process and the following storm assisted in removing the excess sediment causing it to fall to 'normal' levels. The island also exhibits an 'L' shape, with sheltered waters on the inside, possibly acting as a sediment sink due to the low energy in that area. The standard deviation for shorelines and width is reasonably low, as is the standard error of the mean, suggesting that this is the island's normal pattern of geomorphological change. With the increasing shoreline width and corresponding pattern of advance, the island's position appears stable, with little or no migration.

The front and rear shoreline series for Classic 3 displays a uniform pattern of change. Both shorelines appear to advance in a regular manner. The change in the rear shoreline mimics that of the front, although the rear shows greater retreat and continually leapfrogs the front shoreline's rate over the course of the study years, with the shorelines sometimes fluctuating by over 200m in a year. This could be due to a shallow area around the island, with variations in tide or sea level exposing or hiding large volumes of sediment adjacent to the island. The island widths display regular growth suggesting that the island is indeed growing and there is almost certainly a large volume of sediment available in the area. The standard deviations for shorelines and widths, as well as the standard errors, are the highest of any island in this study. This also suggests a high sediment supply, or an external forcing factor, due to the high degree of variability. As this is still in a fetch-limited, low-energy environment, this shows that the island could be highly affected by seasonal storms. As both shorelines mimic each other's patterns and levels of advance/retreat, coupled with the steady rise in shoreline width, there appears to be little or no island migration taking place.

Backbarrier Parallel 1 displays a neutral trend. Island widths show three stable periods, first falling below the original measurement, then rising above and maintaining those levels for several years before falling into a negative state again. The two shorelines however, display an inverse pattern with one shoreline advancing as the other retreats. The front shoreline remains predominantly below the 1984 observation, while the rear remains mainly above with slightly more extreme variations. Both shorelines return to similar levels of advance however. This would suggest that, while the island remains relatively stable, migration towards the rear could be taking place and that overwash from the open-ocean barrier in front is the dominant supply of sediment to the FLBI. Again, there appears to be no correlation between geomorphological change and large storm events, suggesting that regular, consecutive, seasonal storms are most likely the main influence. The standard deviation for the rear is almost double the front, as is the standard error, showing the large degree of variability (although both SEs are still relatively low, suggesting that the island is stable and balanced in

the long-term). The standard deviations for island average width and percentage are also quite high, reflecting the large levels of variation.

Backbarrier Parallel 2 displays a slight negative trend. This occurs on both graphs, with the rear shoreline in a positive position above the front, which remains mainly negative. There is a sharp rise in 2005 that coincides with the major hurricane Emily the month before. This may have caused the transport of high volumes of sediment to the front and rear of the island, explaining this sudden spike in island width. This sediment failed to be incorporated into the island however, as it appears to have been lost the following year, likely due to aeolian processes and overwash removing the unconsolidated load. The island width in 2019 returns to near identical levels as 1984. The two shorelines however, show the rear still in advance with slight retreat from the front, suggesting that the island may be migrating slightly away from the open-ocean barrier. As with BBP1, the standard deviation and standard error for the shorelines show the rear to be roughly double the front, with the standard error still at low levels. Again, the standard deviations for average and percentage widths are relatively high, all of which reflects the high degree of variability in this island's shoreline positions, albeit with a stable geomorphological pattern of change.

Backbarrier Parallel 3 displays the same shoreline patterns as BBP1 and 2, with a negative trend. Despite this, the overall width for 2019 is 102% of the original measurement. CoastSat fails to identify the shorelines until 1992 as they are not yet developed enough. There is a sharp advance in the shorelines from 1992 to 1996, with the rear rise being more extreme. This could be partly to blame for the negative trend observed, even though the island width returns to its original size. The similarities to the other two Backbarrier Parallel Islands continue, with the final shoreline positions showing the rear to be positive and the front negative. Measurements for 2004 to 2006 are absent, meaning the possible effects of Hurricane Emily cannot be viewed. As the shorelines continue their pattern however, this major event appears to have had little or no effect on overall island stability. The standard deviation for the shorelines appears to be higher than the other two islands, with similar values for both front and back, as is the standard error. As there are far less observations due to the later start however, both actually reflect a stable system, with a relatively accurate set of observations. The standard deviation and error for the widths also reflect those seen in the other two islands, again suggesting a highly variable but stable island. Similarly, the ending position of the shorelines, coupled with the similar start and end observations, suggest a stable island retreating from the open-ocean barrier.

The Deltaic FLBI, despite having its first observation in 1985, is missing 21 dates reflecting the difficulty CoastSat had in identifying its shorelines. A greater number of valid shorelines

were available from 2013 onwards, as L8 and S2 provided a higher temporal and spatial resolution, thus increasing the options for each year and providing more accurate images. Issues also occurred with missing transect dates for 1996, 2003 and 2010, as CoastSat left shoreline gaps for those years. Graphs were produced excluding those years to examine errors that could have been introduced by using a mean of two transects instead of three. The normal and corrected graphs show near identical properties and patterns and so, it was decided that the observations on this FLBI were accurate enough to be included. Both shorelines and widths present a positive trend, with the island displaying significant growth over time. The rear side of the island is facing the Rio El Caracol river mouth, where outwash provides a steady sediment supply. While this side represents the greater progradation, the front facing the open lagoon matches its patterns, suggesting a common driver to both sides' geomorphological change. The high standard error and deviation for the rear shoreline reflect the high variability on this side, with many other 'external' factors from the river affecting the geomorphological behaviour. The front displays much lower values, but in a similar ratio, suggesting a 'quiet side'. The high standard error also reflects the comparatively low number of observations when compared to most of the other islands. The widths also display the same high statistics, reinforcing the theme of high variability. As both the width and the shorelines show growth, the island is probably not migrating, but rather gaining size on both sides while remaining geographically stationary.

Inlet 1 displays a negative trend on both graphs. It also displays only a slight similarity in pattern for both shorelines. This could be due to the missing transect data however, as the largest negative rear section coincides with those dates. Additionally, observations were only possible from 2003 onwards as the island did not fully form until then. The southern side for this FLBI was designated as the front, due to the longer fetch and inlet being in that direction. The island appears to be losing most of its area over time, probably due to its proximity to the mouth of the inlet. In this position it would be susceptible to storm generated swell and waves passing through the open inlet. Dredging could also play a role in the island's decline, as attempts to keep the inlet open could affect the sediment supply available. As expected, the standard deviations for the shorelines and the widths are relatively high, reflecting the variability in the island's morphology and the higher energy of the area it lies in. The standard error is also high but this is probably due to having the lowest number of observations of any FLBI in this study.

Inlet 2 shows a negative trend in both graphs and, similar to Inlet 1, begins at an advanced date due to a lack of development. Both shorelines correlate in their development more closely than Inlet 1, with the exception being 2010 to 2011, where there is a large spike in rear (east) advance. This could have been caused by Hurricane Alex in 2010, which hit the southern

section of the study area, moving sediment from the ocean barrier similar to the Backbarrier Parallel islands. Again, this is followed by an immediate sharp drop, re-joining normal trends, probably caused by rapid removal of unconsolidated sediment. The standard deviations are higher for the shorelines compared to Inlet 1; however, they are much lower for the widths, with a slightly lower standard error for shorelines and a far lower one for widths, showing that the island is probably migrating while maintaining a stable pattern of variations in width. This is again supported by the front shoreline displaying regular retreat while the rear advances, coupled with a stable set of width observations.

The Two-Sided FLBI shows a decline on both graphs, with the two shorelines regularly alternating between states of progradation and transgression. This island is unique in that it is positioned perpendicular to the mainland, with a roughly equal fetch north and south. The shoreline alternations reflect this, displaying a general trend but showing a 'back and forth' series of changes for both sides. There is a large deviation in the rear shoreline in 1986, caused by missing data for transect 3 of that year, and skewing the results slightly. However, the low standard error for shorelines and widths, and high number of observations, show that the data series is relatively closely clustered to the mean and is a good representation of the island's pattern of geomorphological change. Overall, it appears that the rear shoreline is more active, fluctuating with a higher range than the front (almost double). The standard deviations for all observations are still reasonably low compared to the other islands, reflecting a stable state. While the width had declined by the most recent date, prior to 2007 (after which begins a slow decline) there appears to be a steady, regular pattern of alternating advance and decline. From 2013 to 2014 there is a sharp year of growth, followed by a sharp fall. Hurricane Emily in 2005 could have caused a temporary deviation from the normal geomorphological state of the island, as it was a major hurricane. Hurricane Ingrid in 2013 could have caused a sediment influx to the island that, similarly to the two Inlet FLBIs, dissipated quickly in the following years. The patterns for the shorelines, coupled with the low standard error, suggest that the island migrates back and forth but has a stable 'point of origin' that it continues to return to.

### *4.3. Qualitative Analysis*

Classic 1 is the largest island in terms of surface area. The southern section appears very unstable and is often reworked into different planforms, hence being excluded from the analysis. While the northern section appears stable through the years, it is still breached occasionally. The north section protrudes north-east over time, eventually forming a spit that curls anticlockwise and will eventually join the main island if its progression continues, closing the small lagoon that it has formed.

Classic 2 shows high levels of breaching at first, with small inlets breaking up the island. These inlets eventually close, joining the sections of the island together. Behind the southern section, a smaller island lies perpendicular to the main island. As time passes this island becomes more established and has begun joining with the larger landform, becoming part of the FLBI in certain years but re-separating in others.

Classic 3 shows clear signs of growth to the east and west. A large amount of sand resides in the shallows around the island, especially in the east. Again, this FLBI breaches quite often but displays a solid, recognisable morphology throughout. A small spit is developing in the north-east section, curling clockwise back towards the main island.

The Backbarrier Parallel 1 FLBI shows little in terms of shoreline evolution. It is also the second-smallest FLBI in this study. It has a slightly sandier area from the south-east to the north-east and displays a very slight migration eastward. It also becomes inundated with water in the centre on occasion, with this lessening as time goes on and the island becomes more established.

As with BBP1, the Backbarrier-Parallel 2 breaches multiple times and over the years this lessens. A large percentage of the island is sandy, showing the surrounding grasses have yet to fully dominate. It appears stable in shape, with a very slight migration eastward.

Backbarrier Parallel 3 begins as a crescent shape, with the shoreline to the east and a small spit to the south. Over time the crescent grows to encircle the central area, closing it off. The centre is often inundated and is still comprised almost entirely of sand. The spit to the south continues to develop directly south.

The Deltaic FLBI displays growth on all sides over time. There are three distinct small ‘lakes’ on the island, and it does not show any sandy shorelines due to its sediment supply originating from the river. There does not appear to be any migration, with the closest landforms showing no signs of joining with this FLBI.

Inlet 1 develops as a string of separate landforms, joining and becoming stable but then decreasing in size over time. It does not appear to migrate, with the 2019 image showing it in the centre of all previous shoreline detections, with a small island to the south-east that was once part of it. It also breaches several times but in the later years small, man-made structures can be seen on the island, perhaps fishing huts.

Inlet 2 appears to migrate slightly south-east. It begins as a small, round planform (the smallest island in this study), but eventually develops a spit in the south. This spit grows anti-clockwise, backing onto the main island and occasionally making a connection, enclosing the small

lagoon that has developed in the centre. It breaches several times through the years, becoming more stable as time passes.

The Two-Sided FLBI appears to lose width over time but becomes more defined, seemingly rising in elevation. It does not show breaching and appears to be quite stable, with no visible migration. A spit is developing to its east in a clockwise direction and coming back on the main island. Of all the FLBIs in the study, this appears to be the most likely candidate for human development.

### *4.4. Conclusions*

Although in a fetch-limited environment, these islands show high levels of variability, often breaching or becoming inundated. Seasonal storm events are the greatest influence on geomorphological change in FLBIs, unlike their oceanic cousins whose morphology is mainly a product of tidal and wave regimes (Mulhern, Johnson and Martin, 2017). Due to the lack of tidal energy reaching the lagoon, consecutive high energy storms exert the greatest influence on the islands' states. There appears to be a steady supply of sediment in the lagoon for the islands to incorporate, with many being supplied by overwash from the open-ocean barrier. The islands in the centre of the lagoon however, rely primarily on the sediment supply immediately adjacent to them for development. While sea level rise does not appear to have impacted the FLBIs currently, in the future it could make this sub-surface supply unavailable to the islands by deepening the lagoon so much that storms and the local wind generated waves cannot influence and transport it. While major storms such as Hurricane Emily coincide with deviations in some island states, all these deviations appear temporary, in line with a previous study on the open-ocean barrier Fire Island, NY in the United States by Hapke et al (2016).

Direct information for the Mexican section of the Laguna Madre is difficult to obtain compared to the Texas section, making the true level of anthropic influence on the FLBIs difficult to gauge. While smaller structures are visible on Inlet 1, there is no guarantee that they will endure consecutive or large storms. With this considered, larger, permanent structures would be highly susceptible to the ethereal nature of the island beneath them and therefore, it would not be appropriate to build on the majority of the FLBIs. However, there may be some that are stable enough due to size, elevation, and evolution (sufficiently evolved or inactive) to erect more permanent structures. Anthropic influences however, may affect the stable nature of these islands, causing them to shift in state and making them more susceptible to external forces, as seen with hard-engineered coastal defences. There are also the ecological consequences of human settlement to consider, as a number of species rely on these islands

to provide shelter, feed, and reproduce (Judd and Tunnell, 2002). Satellite imagery, while providing a reasonable analysis when covering large areas, fails to examine the islands and fine detail. An in-depth field study of these islands (such as the one by Smith, Heap and Nichol (2010) on Tapora Island, North Island, New Zealand), would be useful to further assess their behaviours and long-term resilience.

**References**

Cooper, A., Pilkey, O. and Lewis, D. (2005). Fetch Limited Barrier Islands of Chesapeake Bay And Delaware Bay. Southeastern Geology, 44(1), pp.1-17.

Cooper, J. (2011). Discussion of "Global Distribution and Geomorphology of Fetch-Limited Barrier Islands" by O.H. Pilkey, J.A.G. Cooper, and D.A. Lewis (Journal of Coastal Research, 25[4], 819–837, 2009): Response to Discussion by E.G. Otvos (2010). *Journal of Coastal Research*, 27(2), p.399.

Cooper, J. (2013). Mesoscale geomorphic change on low energy barrier islands in Chesapeake Bay, U.S.A. Geomorphology, 199, pp.82-94.

Cooper, J., Lewis, D. and Pilkey, O. (2007). Fetch-limited barrier islands: Overlooked coastal landforms. GSA Today, 17(3), p.4.

Ehlen, J., Haneberg, W. and Larson, R. (2005). Humans as geologic agents. Boulder, Colorado: Geological Society of America, pp.137-147.

Hapke, C., Plant, N., Henderson, R., Schwab, W. and Nelson, T., 2016. Decoupling processes and scales of shoreline morphodynamics. *Marine Geology*, 381, pp.42-53.

Judd, F. and Tunnell, J. (2002). *The Laguna Madre of Texas and Tamaulipas*. College Station: Texas A & M University.

Mulhern, J., Johnson, C. and Martin, J., 2017. Is barrier island morphology a function of tidal and wave regime?. *Marine Geology*, 387, pp.74-84.

Nhc.noaa.gov. 2020. *National Hurricane Center*. [online] Available at: <https://www.nhc.noaa.gov/> [Accessed 20 October 2019].

Otvos, E. (2010). Definition of Barrier Islands: Discussion of: Pilkey, O.H.; Cooper, J.A.G., and Lewis, D.A., 2009. Global Distribution and Geomorphology of Fetch-Limited Barrier Islands. Journal of Coastal Research, 25(4), 819–837. *Journal of Coastal Research*, 264, pp.787-787.

Pilkey, O., Cooper, J. and Lewis, D. (2009). Global Distribution and Geomorphology of Fetch-Limited Barrier Islands. Journal of Coastal Research, 254, pp.819-837.

Seymour, A., Ridge, J., Newton, E., Rodriguez, A. and Johnston, D. (2019). Geomorphic response of inlet barrier islands to storms. *Geomorphology*, 339, pp.127-140.

Smith, Q., Heap, A. and Nichol, S., 2010. Origin and Formation of an Estuarine Barrier Island, Tapora Island, New Zealand. *Journal of Coastal Research*, 262, pp.292-300.

Stutz, M. and Pilkey, O. (2011). Open-Ocean Barrier Islands: Global Influence of Climatic, Oceanographic, and Depositional Settings. Journal of Coastal Research, 272, pp.207-222.

Usgs.gov. 2020. *USGS.Gov | Science For A Changing World*. [online] Available at: <https://www.usgs.gov/> [Accessed 8 February 2019].

Vos, K., Splinter, K., Harley, M., Simmons, J. and Turner, I. (2019). CoastSat: A Google Earth Engine-enabled Python toolkit to extract shorelines from publicly available satellite imagery. *Environmental Modelling & Software*, 122, p.104528.

Zhang, K. and Leatherman, S. (2011). Barrier Island Population along the U.S. Atlantic and Gulf Coasts. Journal of Coastal Research, 272, pp.356-363.